Molecular Pharmacology Fast Forward. Published on May 7, 2018 as DOI: 10.1124/mol.117.111161
This article has not been copyedited and formatted. The final version may differ from this version.

MOL #111161

THYROID HORMONES ARE TRANSPORT SUBSTRATES AND TRANSCRIPTIONAL REGULATORS OF ORGANIC ANION TRANSPORTING POLYPEPTIDE 2B1

Henriette E. Meyer zu Schwabedissen, Celio Ferreira, Anima M. Schaefer, Mouhssin Oufir, Isabell Seibert, Matthias Hamburger, Rommel G. Tirona

Laboratories of origin:

Biopharmacy, Department Pharmaceutical Sciences, University of Basel, Basel, Switzerland (HEMzS, CF, AMS, IS)

Pharmaceutical Biology, Department Pharmaceutical Sciences, University of Basel, Basel, Switzerland (MO, MH)

Departments of Physiology & Pharmacology and Medicine, University of Western Ontario, London, Ontario, Canada (AMS, RGT)

Downloaded from molpharm.aspetjournals.org at ASPET Journals on April 18, 2024

Molecular Pharmacology Fast Forward. Published on May 7, 2018 as DOI: 10.1124/mol.117.111161
This article has not been copyedited and formatted. The final version may differ from this version.

MOL #111161

Running title: OATP2B1 – an intestinal thyroid hormone transporter

Author of correspondence:

Prof. Dr. med. Henriette E. Meyer zu Schwabedissen, Biopharmacy, Department of Pharmaceutical Sciences, University of Basel, Klingelbergstrasse 50, 4056 Basel, Switzerland, Phone: +41 (0)61-20 71495, Fax: +41 (0)61 20 71498; E-mail: h.meyerzuschwabedissen@unibas.ch

Downloaded from molpharm.aspetjournals.org at ASPET Journals on April 18, 2024

Number of text pages: 30

Number of tables: 2

Number of Figures: 8

Number of References: 46

Number of words in the Abstract: 249

Number of words in the Introduction: 866

Number of words in the Discussion: 1365

List of nonstandard abbreviations: area under the plasma concentration-time curve (AUC); fetal calf serum (FCS); Iodothyronine deiodinases (DIO); Madin Darby Canine Kidney (MDCK); Monocarboxylate Transporter 8 (MCT-8); Organic Anion Transporting Polypeptide (OATP); P-Glycoprotein (P-gp); retinoic X receptor alpha (RXRα); triiodothyronine (T_3); thyroid hormone receptor alpha (TRα); thyroid hormone (TH); thyroid hormone receptor beta (TRβ); thyroxine (T_4); thyroid-stimulating hormone (TSH);

Molecular Pharmacology Fast Forward. Published on May 7, 2018 as DOI: 10.1124/mol.117.111161
This article has not been copyedited and formatted. The final version may differ from this version.

Abstract

Levothyroxine replacement therapy forms the cornerstone of hypothyroidism management. Variability in levothyroxine oral absorption may contribute to the well-recognized large interpatient differences in required dose. Moreover, levothyroxine-drug pharmacokinetic interactions are thought to be caused by altered oral bioavailability. Interestingly, little is known regarding the mechanisms contributing to levothyroxine absorption in the gastrointestinal tract. Here, we aimed to determine whether the intestinal drug uptake transporter Organic Anion Transporting Polypeptide 2B1 (OATP2B1) may be involved in facilitating intestinal absorption of thyroid hormones. We also explored whether thyroid hormones regulate OATP2B1 gene expression. In cultured MDCKII-OATP2B1 cells and in OATP2B1-transfected Caco-2 cells, thyroid hormones were found to inhibit OATP2B1-mediated uptake of estrone 3-sulfate. Competitive counter-flow experiments evaluating the influence on the cellular accumulation of estrone 3-sulfate in the steady-state, indicated that thyroid hormones were substrates of OATP2B1. Additional evidence that thyroid hormones were OATP2B1 substrates was provided by OATP2B1-dependent stimulation of thyroid hormone receptor activation in cell-based reporter assays. Bidirectional transport studies in intestinal Caco-2 cells showed net absorptive flux of thyroid hormones, which was attenuated by the presence of the OATP2B1 inhibitor, atorvastatin. In intestinal Caco-2 and LS180 cells, but not in liver Huh-7 or HepG2 cells, OATP2B1 expression was induced by treatment with thyroid hormones. Reporter genes assays revealed thyroid hormone receptor α-mediated transactivation of the *SLCO2B1* 1b and the *SLCO2B1* 1e promoters. We conclude that thyroid hormones are substrates and transcriptional regulators of OATP2B1. These insights provide a potential mechanistic basis for oral levothyroxine dose variability and drug interactions.

Downloaded from molpharm.aspetjournals.org at ASPET Journals on April 18, 2024

Molecular Pharmacology Fast Forward. Published on May 7, 2018 as DOI: 10.1124/mol.117.111161
This article has not been copyedited and formatted. The final version may differ from this version.

Introduction

Thyroid hormone (TH) homeostasis is essential for physiological energy metabolism. Accordingly, alterations are linked to a variety of diseases. With a prevalence of about 4-5% in European or American populations, hypothyroidism (overt and subclinical) is among the most common diagnoses in endocrinology (Garmendia Madariaga et al., 2014; Hollowell et al., 2002). TH homeostasis is tightly regulated by multiple mechanisms including those, which control tissue uptake and cellular bioactivation. Thyroxine (T_4) is metabolized by intracellular iodothyronine deiodinases which produce biologically active triiodothyronine (T_3) or inactive reverse triiodothyronine (rT_3) (Kohrle, 2007). In order to signal transcription, T_3 binds to intracellular thyroid hormone receptors (TRs) (Mondal et al., 2016). The therapeutic management of hypothyroidism usually involves oral substitution with L-thyroxine (T_4). However, oral absorption of L-thyroxine is highly variable and known to be affected by various factors including gastric pH, or food-drug interactions (Ianiro et al., 2014). Furthermore, it is known that efficient L-thyroxine absorption from the intestinal lumen occurs in restricted segments of the gastrointestinal tract, namely the duodenum and jejunum (Ianiro et al., 2014).

Intestinal solute transfer is mainly mediated by passive diffusion and active transport by membrane proteins. Several well-known drug-drug interactions result in reduced L-thyroxine bioavailability. For example, proton pump inhibitors (PPIs) alter the ionization status of L-thyroxine in the gut due to increased gastric pH, while iron or calcium supplements may form non-absorbable chelates or complexes with THs (Centanni et al., 2006). Interestingly, a population based retrospective study observed changes in TSH levels, a marker for TH activity, to be associated with co-treatment with statins (Irving et al., 2015). Furthermore, an acute impact of ciprofloxacin or rifampin on intestinal absorption of L-thyroxine was shown, where ciprofloxacin significantly reduced T_4 area under the plasma concentration-time curve (AUC) by 39%, while

Downloaded from molpharm.aspetjournals.org at ASPET Journals on April 18, 2024

Molecular Pharmacology Fast Forward. Published on May 7, 2018 as DOI: 10.1124/mol.117.111161
This article has not been copyedited and formatted. The final version may differ from this version.

rifampin significantly increased T_4 AUC (25%) (Goldberg et al., 2013). These later findings suggest that L-thyroxine-drug interactions may also result from mechanisms involving facilitated cellular entry or efflux (Riley et al., 2016).

With the discovery that MCT-8 (*SLC16A2*) genetic mutations cause Allan-Herndon-Dudley syndrome, a severe psychomotor retardation associated with TH dysregulation (Visser et al., 2011), it has become widely accepted that transporters are critically involved in the regulation of TH homeostasis and function (Bernal et al., 2015). Additional transporters have been reported to interact with THs, including members of the Organic Anion Transporting Polypeptides (OATPs) (van der Deure et al., 2010). Within this protein family, OATP1C1 appears to be highly active and specific for TH transport, though it is only expressed at the blood-brain barrier and in the testis (Pizzagalli et al., 2002; Sugiyama et al., 2003). In addition, the hepatic transporters OATP1B1 and OATP1B3 have been reported to mediate cellular uptake of iodothyronine sulfates (van der Deure et al., 2008), thereby contributing to hepatic TH elimination. With regard to intestinal L-thyroxine absorption, the above mentioned OATPs appear of minor relevance due to their expression profile. In contrast, OATP1A2 was reported to be expressed in intestine (Glaeser et al., 2007) and to recognize THs as substrates (Fujiwara et al., 2001). However, intestinal OATP1A2 expression could not be subsequently confirmed, accordingly the transporter is mainly considered important for blood-brain transfer (Lee et al., 2005; van der Deure et al., 2010).

A leading candidate for an intestinal TH-transporter is OATP2B1 (*SLCO2B1*). This sodium-independent uptake transporter is expressed in enterocytes and assumed to significantly influence oral drug absorption (Drozdzik et al., 2014; Kullak-Ublick et al., 2001; Tamai et al., 2000). While most studies supported localization of OATP2B1 at the apical membrane of the enterocyte, its polarized cellular localization is matter of debate as a basolateral sorting has recently been proposed (Keiser et al., 2017; Kobayashi et al., 2003). Despite that OATP2B1 is known to mediate cellular

Downloaded from molpharm.aspetjournals.org at ASPET Journals on April 18, 2024

Molecular Pharmacology Fast Forward. Published on May 7, 2018 as DOI: 10.1124/mol.117.111161
This article has not been copyedited and formatted. The final version may differ from this version.

uptake of various exogenous compounds including statins (Koenen et al., 2011), it is less certain whether this transporter is also involved in intestinal absorption of THs, as there are conflicting data. Interestingly, both studies reporting data on this used a similar experimental model involving *Xenopus laevis* oocytes expressing OATP2B1 (Kullak-Ublick et al., 2001; Leuthold et al., 2009). There are several transcription start site (TSS) variants of OATP2B1 (Pomari et al., 2009), which are all regulated by their own distinct promoter (1a to 1e, Figure 8A). Of these five variants the OATP2B1 isoform 1B (using exon 1b as TSS) encodes for the original full-length protein and is the major form expressed in duodenum. All other variants that are transcriptionally controlled by different promoter regions, encode for the same shortened protein lacking 22 amino acids at the N-terminus. This short variant exhibits transport of estrone 3-sulfate and rosuvastatin comparable to the full-length OATP2B1 isoform 1B. For the OATP2B1- 1E variant liver enriched expression and regulation by HNF4α has recently been reported (Knauer et al., 2013). In this study, we investigated the functional and regulatory interplay of TH and the uptake transporter OATP2B1. Using cells overexpressing OATP2B1, we examined the impact of THs on cellular accumulation of the known OATP2B1-substrate estrone 3-sulfate. Cellular accumulation studies were supplemented by counterflow experiments, and an assessment of the influence of OATP2B1 on the transactivation of TRβ. Finally, we used the intestinal Caco-2 cell model to study transcellular TH transport as well as regulation of OATP2B1 expression.

Downloaded from molpharm.aspetjournals.org at ASPET Journals on April 18, 2024

Materials and Methods

Cell culture. All cell lines were kept at 37°C in a humidified atmosphere supplemented with 5% CO_2. The cell lines Caco-2 (ATCC# HTB37), HepG2 (ATCC# HB-8065), HeLa (ATCC# CCL-2) and MDCKII (ATCC# CRL-2936) were originally obtained from American Tissue Culture Collection. Huh-7 cells (clone JCRB0403) were purchased from the Japanese Collection of Research Bioresources. Primary human renal proximal tubular epithelial cells (RPTEC) were

Molecular Pharmacology Fast Forward. Published on May 7, 2018 as DOI: 10.1124/mol.117.111161
This article has not been copyedited and formatted. The final version may differ from this version.

purchased from Ruwag Life science (Bettlach, Switzerland). LS180 cells (Cat# 87021202) were commercially obtained from Sigma-Aldrich (Buchs, Switzerland). The OATP2B1 overexpressing cell line MDCKII-OATP2B1 was generated and characterized as described elsewhere (Grube et al., 2006). DMEM supplemented with 10% FCS and 1% GlutaMAX™ (Thermo Fisher Scientific, Zug, Switzerland) were used as culture medium for Caco-2, HeLa, HepG2, Huh-7, and MDCKII cells. In case of MDCKII-OATP2B1 the medium was supplemented with 0.25 mg/ml Hygromycin B for continuous selection. DMEM supplemented with 1% GlutaMAX™, 10% FCS, and 1% non-essential amino acids was the culture medium for LS180 cells. The RPTECs were kept in optimized Clonetics™ REGM™ renal epithelial cell growth medium supplemented as recommended by the manufacturer (Lonza, Basel, Switzerland).

***In silico* scan for potential thyroid hormone receptor binding sites.** The previously published sequences of the *SLCO2B1* 1b promoter and the *SLCO2B1* 1e promoter (Knauer et al., 2013) were screened for potential TR binding sites using the open access program NUBIScan version 2.0 (www.nubiscan.unibas.ch). The underlying algorithm is a joining of weighted distribution matrices of nucleotide hexamer half sites as published by Podvinec *et al*. (Podvinec et al., 2002). The herein used search matrix was generated based on previously described specific DNA sequence binding pattern for TRs (Ayers et al., 2014).

Immunofluorescent staining. Cells were seeded on cover slides at a density of 75,000 cells/ well in 12-well plates. After reaching 90% confluence, cells were fixed with ice-cold methanol:aceton (1:2) for 15 minutes, then permeabilized with 0.2% Tween 20-PBS, and then incubated with 5%-FCS-1% BSA-PBS before adding the anti-OATP2B1-antiserum (1:100) (Grube et al., 2006) for incubation over night at 4°C. After several washes with PBS, the secondary antibody anti-rabbit Alexa Fluor® 488 (Life Technologies, Thermo Fisher Scientific) was added for 1 hour. Prior to mounting the cells with Roti®-Mount FluorCare containing DAPI for nuclei

Downloaded from molpharm.aspetjournals.org at ASPET Journals on April 18, 2024

Molecular Pharmacology Fast Forward. Published on May 7, 2018 as DOI: 10.1124/mol.117.111161
This article has not been copyedited and formatted. The final version may differ from this version.

staining the cells were washed with PBS. Staining was detected using the Leica DMi8 Microscope (Leica Microsystems, Heerbrugg, Switzerland).

Quantitative Real-time PCR analysis. Caco-2, LS180, Huh-7 and HepG2 cells were cultured at confluence in 6-well plates and then treated with 100 nM thyroxine (T_4) or 100 nM triiodothyronine (T_3). After 48 h of treatment, total RNA was extracted using TRIzol reagent (Thermo Fisher Scientific). The quality of the RNA was determined using the Agilent Bioanalyzer 2100 (Agilent, Santa Clara, CA, USA) and concentration was measured by spectrophotometry (GE Nanovue Plus, GE, Baie d'Urge, QC, Canada). cDNA was synthesized using the Multiscribe™ Reverse Transcriptase (Applied Biosystems distributed by LuBioScience, Lucern, Switzerland). Human tissue RNAs were purchased from AMS Biotechnology (Bioggio-Lugano, Switzerland) or isolated from RPTEC, Caco-2, or Huh-7 using pegGold RNA Pure™ (Axon Lab, Baden-Dättwil, Switzerland) following the manufacturers protocol. The High-Capacity cDNA Reverse Transcription Kit (Life Technologies, distributed by LuBioScience) was used for reverse transcription. The amount of mRNA was quantified using the ViiA™7 Real-Time PCR System and commercially available TaqMan® gene expression assays (LuBioScience) for thyroid hormone receptor beta (TRβ, Hs00230861), thyroid hormone receptor alpha (TRα, Hs00268470_m1), iodothyronine deiodinase 1 (DIO1, Hs00174944_m1), and 18S ribosomal RNA (18S rRNA, 4319413E). The amount of the *SLCO2B1* isoforms 1B and 1E were analyzed using the SYBR® Green PCR Master Mix (LuBioScience) and the following primers *SLCO2B1*_1B_for 5'-GGCTGGAGCTCACTGCAC-3', *SLCO2B1*_1E_for 5'-TGGGATTGAAGCTTCAGGGAG-3', and *SLCO2B1*_1B/1E_rev 5'-CACTGTGGAAATGGAGCTC-3' as previously reported by Knauer *et al.* (Knauer et al., 2013). In cells, DIO1 and ABCB1 were quantified using the primers DIO1_for 5'-TTCAGCACCAGTGGCCTATT-3', DIO1_rev 5'-ACGACTGAGCTAGGGGGTCT-3', P-gp_for

Downloaded from molpharm.aspetjournals.org at ASPET Journals on April 18, 2024

Molecular Pharmacology Fast Forward. Published on May 7, 2018 as DOI: 10.1124/mol.117.111161
This article has not been copyedited and formatted. The final version may differ from this version.

5'-GTCCCAGGAGCCCATCCT-3' and P-gp_rev 5'-CCCGGGTGTTGTCTCCAT-3'. Data were analyzed by the ΔΔCT method, where CT values of the gene of interest were normalized to that of 18S rRNA detected in the same sample (ΔCT). The ΔCT values of each sample were referred to the mean ΔCT-value of the indicated control (ΔΔCT).

Transport studies using MDCKII-OATP2B1 cells. For inhibition studies and competitive counter-flow experiments MDCKII or MDCKII-OATP2B1 cells were seeded at a density of 50,000 cells/ well in 24-well plates. One day after seeding, cells were stimulated with 2.5 mM sodium-butyrate for 24 h. For inhibition studies, cells were washed with pre-warmed PBS prior to the 5 min incubation with estrone 3- sulfate (E_1S) diluted in incubation buffer [142 mM NaCl, 5 mM KCl, 1 mM KH_2PO_4, 1.5 mM $CaCl_2$, 1.2 mM $MgSO_4$, 5 mM glucose and 12.5 mM HEPES]. E_1S was used at a concentration of 0.1 µM containing 100,000 dpm/well [^{3}H]-estrone 3- sulfate (Hartmann Analytic, Braunschweig, Germany), supplemented with the respective concentration of the tested inhibitor namely T_4, T_3, rT_3, thyroxine 4-O-β-D-glucuronide (T_4G) (all obtained from Sigma-Aldrich). Atorvastatin [1 or 10 µM] was used as control. After washing the cells three times with ice cold PBS cells were lysed in 200 µl 10% SDS-5 mM EDTA. Cellular accumulation of the radiolabeled substrate was determined after diluting the cell lysate in 2 mL of scintillation cocktail (Rotiszint® eco plus; Carl Roth AG, Arlesheim, Switzerland) and measured using a liquid scintillation β-counter (Tri-carb 2900 TR; TOPLAB, Rickenbach, Switzerland). Competitive counter-flow experiments were performed as described by Harper *et. al.* (Harper and Wright, 2013). One day after seeding, the cells were washed once with pre-warm PBS and exposed to Krebs-Henseleit buffer (KHB; 118 mM NaCl, 25 mM $NaHCO_3$, 1.2 mM KH_2PO_4; 2.5 mM $CaCl_2$, 1.2 mM $MgSO_4$, 11 mM Glucose, 4.7 mM KCl; pH 5.5) containing [^{3}H]-estrone 3-sulfate (E_1S, 6.06 nM/well with 100,000 dpm/well) for 30 minutes to equilibrate. After reaching steady-state conditions, the supernatant was removed and replaced by KHB containing [^{3}H]-E_1S supplemented

Downloaded from molpharm.aspetjournals.org at ASPET Journals on April 18, 2024

Molecular Pharmacology Fast Forward. Published on May 7, 2018 as DOI: 10.1124/mol.117.111161
This article has not been copyedited and formatted. The final version may differ from this version.

with the test compounds namely E_1S (50 µM), atorvastatin (30 µM), camptothecin (1 mM), T_4 (25 µM), T_3 (10 µM), rT_3 (1 mM), or T_4G (400 µM). After one-minute incubation the cells were washed with ice-cold PBS, and amount of radiolabel in lysed cells was determined as described above.

Transport studies using transiently transfected Caco-2 cells. Caco-2 cells were seeded at a density of 75,000 cells/well in 24-well plates. One day after seeding the cells were transfected with 500 ng/well pEF6-control or OATP2B1-pEF6 using 2 µl/ µg DNA jetPRIME® transfection reagent (Polyplus transfection,-Chemie Brunschwig AG, Basel, Switzerland). The day after transfection transport experiments were conducted as described in detail above.

Cell-based reporter gene assays. In order to test the influence of the uptake transporter on the intracellular function of T_3 and T_4 MDCKII or MDCKII-OATP2B1 cells were transfected with a reporter gene construct containing the firefly luciferase gene under the control of the 5' untranslated region of the iodothyronine deiodinase 1 gene (DIO1-pGL3basic) and pRL-TK encoding for the Renilla luciferase as transfection control. For cell-based reporter gene assays testing the transactivation of the *SLCO2B1* 1e and *SLCO2B1* 1b promoters, the respective reporter gene constructs in pGL3basic (Knauer et al., 2013) were transfected into HeLa cells. In addition to the reporter gene constructs, the cells were transfected with eukaryotic expression vectors (pEF6-V5/HIS, Invitrogen) encoding for the nuclear receptor thyroid hormone receptor beta (TRβ), thyroid hormone receptor alpha (TRα) and/or its heterodimerization partner retinoic X receptor alpha (RXRα). In total, 25 ng pRL-TK, 250 ng of TRβ-pEF6, TRα-pEF6 and/or RXRα-pEF6 and/or pEF6 as control, and 250 ng of the pGL3basic plasmid were transfected in each well. MDCKII or MDCKII-OATP2B1 cells were seeded at a density of 40,000 cells/well in a 24-well plate, after 24 hours the cells were transfected using 1.5 µl/µg DNA of the jetPRIME® transfection reagent (Polyplus transfection). HeLa cells were seeded at a density of 50,000 cells/well in 24-well

Downloaded from molpharm.aspetjournals.org at ASPET Journals on April 18, 2024

Molecular Pharmacology Fast Forward. Published on May 7, 2018 as DOI: 10.1124/mol.117.111161
This article has not been copyedited and formatted. The final version may differ from this version.

plates, and were transfected using 2.5 µl/µg DNA of the jetPRIME® transfection reagent (Polyplus transfection). The day after, the cells were treated for 24 h with 10 µM T_3 or 10 µM T_4. Subsequently the cells were lysed in 100 µl passive lysis buffer, then the firefly and Renilla luciferase activities were assessed in 20 µl of the lysate using the Dual-Luciferase® Reporter Assay System (Promega, Duebendorf, Switzerland) and the infinite® 200 Pro (Tecan, Maennedorf, Switzerland) according to the manufacturer's instruction. Activity of firefly luciferase was normalized to that of Renilla.

Western Blot analysis. For determination of protein content cells were lysed in 5 mM Tris-HCl (pH 7.4) supplemented with protease inhibitors (diluted 1:100; Protease Inhibitors Cocktail; Sigma-Aldrich). After three cycles of freezing in liquid nitrogen and thawing in a 37°C water bath, the cell lysate of MDCK cells was centrifuged at 100,000 x g (30 min at 4°C) for crude membrane enrichment. The resulting pellet was suspended in 5 mM Tris-HCl supplemented with protease inhibitors. For cultured Caco-2 cells, we applied the total cell lysate to immunoblotting. After adding 5 x Laemmli buffer, the samples were heated for 30 minutes to 65°C prior to separation by 10% SDS-PAGE. The separated proteins were electrotransferred to a nitrocellulose membrane using a TANK blotting system (Bio-Rad, Cressier, Switzerland). Prior to incubation with the respective antibodies anti-OATP2B1 rabbit polyclonal (Grube et al., 2006), or goat polyclonal anti-β-actin (sc-1616, Labforce, Muttenz, Switzerland), the membranes were blocked with 5%-fetal calf serum in Tris-buffered saline containing 0.1% Tween 20 (TBST) for at least an hour at room temperature. After several washing steps with TBST the membranes were incubated with the respective horseradish peroxidase-labelled secondary antibody (dilution to 1:2000, Bio-Rad). Immobilized secondary antibody was visualized and digitalized using the Western ECL Substrate (Thermo Fisher Scientific) and the ChemiDoc™ MP System (Bio-Rad), respectively. Analysis was performed using the Image Lab software (Version 4.1; Bio-Rad).

Downloaded from molpharm.aspetjournals.org at ASPET Journals on April 18, 2024

Molecular Pharmacology Fast Forward. Published on May 7, 2018 as DOI: 10.1124/mol.117.111161
This article has not been copyedited and formatted. The final version may differ from this version.

Transwell transport of thyroid hormones. Transepithelial solute flux studies were performed as previously published by Hubatsch *et al.* (Hubatsch et al., 2007). Briefly, Caco-2 cells were seeded at a density of 3×10^5 cells/well onto polycarbonate membranes with 0.4 µm pore size inserted in 12-well plates (Chemie Brunschwig). Caco-2 cells were cultivated for at least 14 days with medium change every second day, and until reaching a transepithelial electrical resistance (TEER) value of at least 200 Ω/cm. Integrity of the monolayer was tested after assessment of transport using 0.1 mg/mL lucifer yellow (Sigma-Aldrich). Transport experiments were performed using KHB. In detail, after washing the cells with PBS, Caco-2 cells were pre-equilibrated for 20 minutes at 37C° with KHB. The apical compartment was filled with 0.5 ml and the basolateral compartment with 1.5 ml of KHB. 10 µM T_3 or 10 µM T_4 was applied to the donor compartment. Inhibition of OATP2B1 was achieved by application of 10 µM atorvastatin (USP, Basel, Switzerland) on the apical site. Accumulation in the acceptor compartment and remaining amount in the donor compartment was quantified in 200 µl aliquots taken at 30 minutes and replaced with KHB buffer. At 60 minutes a second aliquot was taken. Both apical and basolateral KHB samples were stored in glass vials (to avoid long-term nonspecific adsorption) below -65°C prior to quantification by UHPLC-MS/MS as described below. The permeability coefficient (P_{app}) was calculated as previously described (Hubatsch et al., 2007). The determined unidirectional apparent permeability coefficients in A (apical) to B (basal) or B to A direction was used to calculate the uptake ratio. In accordance to the commonly used efflux ratio, the uptake ratio was calculated as follows:

$$uptake - ratio = \frac{P_{app}\,(A\ to\ B)}{P_{app}(B\ to\ A)}$$

Triiodothyronine and thyroxine quantification by UHPLC-MS/MS. For the quantification of T_3 and T_4 in the range of 30-3,000 ng/mL specific ultra-high-performance liquid chromatography coupled to tandem mass spectrometry (UHPLC-MS/MS) methods were developed. For both T_3

Downloaded from molpharm.aspetjournals.org at ASPET Journals on April 18, 2024

Molecular Pharmacology Fast Forward. Published on May 7, 2018 as DOI: 10.1124/mol.117.111161
This article has not been copyedited and formatted. The final version may differ from this version.

and T_4, seven calibration standards (calibrators) and three levels of quality controls (QCs) in KHB at low (QCL 90 ng/mL), medium (QCM 1500 ng/mL), and high (QCH 2400 ng/mL) concentrations were prepared by serial dilution of the respective working solution (100 µg/mL in methanol for both T_3 and T4). The first concentration (30 ng/mL) of the calibrators was defined as lower limit of quantification (LLOQ), and the highest concentration (3000 ng/mL) as upper limit of quantification (ULOQ). Calibrators and QCs were stored in aliquots in polypropylene tubes at below - 65°C until analysis. $^{13}C_6$-T_3 and $^{13}C_6$-T_4 (dissolved to 1,000 ng/mL in methanol Sigma-Aldrich) were used as internal standards (IS) for T_3 and T_4, respectively. To 20 µL of the KHB samples from Transwell® studies, 100 µL of each IS, 200 µL Bovine Serum Albumin (BSA) solution (60 g/L), and 700 µL of ice-cold acetonitrile (ACN) were added. The mixture was briefly vortexed, mixed for 10 minutes at 1 400 rpm and room temperature, and then centrifuged for 20 minutes at 13 200 rpm and 10ºC. The supernatant was transferred into a 96-deep well plate, dried under heated nitrogen gas flow (30-50°C; Evaporex EVX-96, Apricot Designs, Monovia, CA, USA), and reconstituted with 200 µL of injection solvent (35% eluent A and 65% eluent B, eluent A: 0.1% formic acid in water, eluent B: 0.1% formic acid in ACN) under shaking (1,500 rpm) for 45 min at room temperature. Subsequently, each sample was transferred into a 300 µL glass insert of a HPLC vial before injection into the UPLC-MS/MS system in full loop mode (5 µL). Quantification was performed using an UPLC HSS T3 column on an Acquity UPLC system consisting of a binary pump, an autosampler set at 10ºC, and a column heater set at 45ºC, which was coupled to an Acquity TQD tandem mass spectrometer (all Waters Corp., Milford, MA, USA). The mobile phase consisted of eluents A and B. Chromatographic separation was performed at a flow rate of 0.5 mL/min with the following gradient: 0-1 min, B 5%; 1-5 min, B 5-100%; 5-6 min, B 100%; 6-6.01 min, B 100-5%; 6.01-7 min, B 5%. In addition to the above mentioned injection solvent and eluents, the weak and strong wash solvents were water-ACN (50:50, v/v) containing

Downloaded from molpharm.aspetjournals.org at ASPET Journals on April 18, 2024

Molecular Pharmacology Fast Forward. Published on May 7, 2018 as DOI: 10.1124/mol.117.111161
This article has not been copyedited and formatted. The final version may differ from this version.

0.2% trifluoroacetic acid (TFA), and ACN-isopropanol-acetone (40:40:30, v/v/v) containing 0.2% TFA, respectively. The seal wash solvent consisted of a water-ACN mixture (90:10, v/v). MRM detection was performed with electrospray ionization in positive ion mode (ESI+). Nitrogen was used both as desolvation and nebulization gas. Argon was used as collision gas. MS/MS parameters were generated using Waters IntelliStart software followed by manual optimization. The optimized parameters are summarized in table 1.

Statistical analysis. Data are presented as mean ± SD. Data analysis was performed using the GraphPad Prism software 6.04 (GraphPad Software, San Diego, CA, USA.) and Microsoft Excel (Microsoft, Redmond, WA, USA.). $p \leq 0.05$ were considered as statistically significant.

Results

Influence of thyroid hormones on OATP2B1 transport activity. In a first approach, we tested the influence of T_4 and its metabolic products, namely T_3, rT_3, and T_4G (Figure 2A) on OATP2B1-mediated uptake of the known substrate estrone 3-sulfate (E_1S) using OATP2B1 expressing MDCKII cells. Expression of OATP2B1 (isoform 1B) in the cell model was verified by immunofluorescence microscopy (Figure 1A) and Western blot analysis (Figure 1B) showing localization of OATP2B1 at the plasma membrane of over-expressing MDCKII-OATP2B1 cells. As shown in Figure 2B-E, all of the tested compounds significantly inhibited OATP2B1 transport function, thereby providing the first evidence of an interaction of thyroid hormones with this membrane transporter. OATP2B1 function was potently inhibited by T_4 (IC_{50} 2.43 µM, CI 2.91 to 3.08) and T_3 (IC_{50} 0.51 µM CI 0.39 to 0.64), while rT3 (IC_{50} 14.88 µM CI 12.16 to 18.21) and T4G (IC_{50} 44.55 µM CI 36.07 to 55.03) exhibited lower inhibitory potency. Inhibition of OATP2B1 by the known OATP2B1 substrate, atorvastatin, served as a positive control of the experimental system (Figure 1C). The influence of thyroid hormone derivatives was also tested in Caco-2 cells transiently transfected with OATP2B1-pEF6 for overexpression of the transport protein. Using this

Downloaded from molpharm.aspetjournals.org at ASPET Journals on April 18, 2024

Molecular Pharmacology Fast Forward. Published on May 7, 2018 as DOI: 10.1124/mol.117.111161
This article has not been copyedited and formatted. The final version may differ from this version.

cell model, we also observed inhibition of OATP2B1 mediated cellular accumulation of E_1S for T_4 (IC_{50} 4.81 µM, CI 3.65 to 6.34), T_3 (IC_{50} 0.97 µM CI 0.61 to 1.53), rT_3 (IC_{50} 16.10 µM CI 11.44 to 22.65), and T_4G (IC50 57.21 µM CI 38.11 to 85.89). Notably, the transport rate of estrone 3-sulfate in OATP2B1-transfected Caco-2 cells was lower than that observed for stably transfected MDCKII-OATP2B1 cells (mean transport rate ± SD; fmol µg protein^{-1}min^{-1}; Caco-2-OATP2B1 vs. MDCKII-OATP2B1; 0.268 ± 0.055 *vs.* 1.226 ± 0.086; n=3 independent replicates, each in biological triplicates; $p<0.05$ Ordinary one-way ANOVA with Turkey's multiple comparison test).

Competitive Counter-flow transport studies with thyroid hormones in OATP2B1-expressing cells. Subsequently, competitive counter-flow experiments were conducted to determine, whether the observed inhibition is due to transport of the tested thyroid hormone derivative. Counter-flow was assessed in MDCKII-OATP2B1 cells at equilibrium, which was reached after 30 minutes of incubation with estrone 3-sulfate (compare Figure 3A). An examination of the remaining amount of radiolabeled [^{3}H]-E_1S in cells exposed to T_4 (25 µM), T_3 (10 µM), and rT_3 (1 mM) revealed significantly lower levels of the radiolabel compared to cells exposed to DMSO vehicle control (mean percent of DMSO control ± SD; T_4: 39.41 ± 9.93 %, T_3: 40.34 ± 10.37 %; rT_3 57.20 ± 15.37 %; one-way ANOVA with Dunnett´s multiple comparison test; $p<0.05$), suggesting that these compounds are OATP2B1 substrates. In this assay, the known OATP2B1 substrates atorvastatin (30 µM; 28.33 ± 6.17 %) and estrone 3-sulfate (50 µM; 42.31 ± 8.26 %) expectedly reduced intracellular E_1S after addition in the steady-state. Lastly, T_4G (400 µM; 80.70 ± 33.70 %) or camptothecin (97.71 ± 14.07 %) did not affect cellular E_1S equilibrium (Figure 3B), indicating that these compounds were not substrates of OATP2B1.

Influence of OATP2B1 transport function on intracellular thyroid hormone effects. To provide additional evidence for OATP2B1 transport of thyroid hormones, we tested the impact of OATP2B1 expression on intracellular thyroid hormone signaling. MDCKII or MDCKII-

Downloaded from molpharm.aspetjournals.org at ASPET Journals on April 18, 2024

Molecular Pharmacology Fast Forward. Published on May 7, 2018 as DOI: 10.1124/mol.117.111161
This article has not been copyedited and formatted. The final version may differ from this version.

OATP2B1 cells were used for cell-based reporter gene assays that examined transactivation of the human iodothyronine deiodinase 1 (DIO1)-promoter (insert Figure 4). With overexpression of the OATP2B1 transporter, transactivation of the DIO1 promoter was significantly enhanced by both T_3 and T_4 with co-transfection of thyroid hormone receptor beta (TRβ) with or without retinoid X receptor alpha (RXRα) (Figure 4A, 4B). Thyroid hormones did not activate the DIO1- promoter in both cell lines transfected with just RXRα (Figure 4C), indicating the signal enhancement was TRβ-dependent. It is notable that the transfection efficacy in MDCKII is much lower than that of HepG2 or HeLa cells in cell based reporter gene assays conducted in our laboratory. This in part explains the lower transactivation of the DIO1-promoter with about 3-fold, as we usually see a transactivation of about 5-6 fold compared to vector control, in those experiments with cells better accessible by transfection.

Expression of OATP2B1 and thyroid hormone receptor β in human tissues and cellular models. Different tissues and commonly used cellular models of those organs were analyzed by real-time PCR to determine endogenous expression of the transporter OATP2B1 isoform 1B, OATP2B1 isoform 1E, the thyroid hormone receptor β (TRβ), the thyroid hormone receptor α (TRα), and iodothyronine deiodinase 1 (DIO1). The DIO1 was only observed in liver kidney, and in Caco-2, HepG2, Huh-7 and RPTECs but not in LS180 cells (mean expression ± SD, relative to liver, Caco-2 *vs.* LS180 *vs.* Huh-7 *vs.* HepG2 *vs.* RPTEC, DIOI: 0.779 ± 0.313 *vs.* not detected *vs.* 0.038 ± 0.003 *vs*. 0.162 ± 0.027 *vs.* 0.006 ± 0.006, data not shown). As shown in Figure 5A and 5B, the mRNA of TRα or TRβ was observed in all tissues studied. Examination of the mRNA expression of the OATP2B1 isoforms verified the previous observation of isoform 1B as enriched in the intestine, while isoform 1E (Figure 5E) being predominantly expressed in liver (Figure 5F) (Knauer et al., 2013). For all genes examined in different cell models, highest expression levels were observed in intestinal Caco-2 cells compared to LS180, Huh-7, HepG2, and

Downloaded from molpharm.aspetjournals.org at ASPET Journals on April 18, 2024

Molecular Pharmacology Fast Forward. Published on May 7, 2018 as DOI: 10.1124/mol.117.111161
This article has not been copyedited and formatted. The final version may differ from this version.

RPTEC (mean expression ± SD, relative to liver, Caco-2 *vs.* LS180 *vs.* Huh-7 *vs.* HepG2 *vs.* RPTEC, TRα: 36.266 ± 7.289 *vs.* 28.116 ± 6.395 *vs.*12.942 ± 3.582 *vs.*2.815 ± 0.374 *vs.* 7.531 ± 1.686; TRβ: 4.521 ± 1.224 *vs.* 4.321 ± 0.372 *vs.* 4.614 ± 0.315 *vs.* 1.022 ± 0.162 *vs.* 1.384 ± 0.157, OATP2B1-1B: 149.599 ± 66.648 *vs.* not detected *vs.* 14.071 ± 4.627 *vs.* 5.358 ± 0.956 *vs.* 0.145 ± 0.074 and OATP2B1-1E: 9.278 ± 2.381 *vs.* 3.553 ± 0.334 *vs.* 0.297 ± 0.073 *vs.* 0.222 ± 0.083 *vs.* 0.002 ± 0.001; Figure 5C, D, G, H), thereby supporting further use of Caco-2 cells for *in vitro* studies on the interactions of OATP2B1 and thyroid hormones.

Quantification of transcellular transport of thyroxine and triiodothyronine in Caco-2 cells. Transcellular flux of T_4 or T_3 was assessed in differentiated Caco-2 cells cultured in Transwells®. The amount of T_4 and T_3 in the apical or basal compartment was quantified by UHPLC-MS/MS. Solute flux studies in the apical (A) to basolateral (B) direction revealed that T_4 exhibits intermediate, while T_3 shows low permeability as the P_{app} was below 3.3 x 10^{-6} cm/s (mean $P_{app\ (A-B)}$ ± SD [cm/s], T_4: 3.70 x 10^{-6} ± 0.17 x 10^{-6}; T_3: 2.75 x 10^{-6} ± 7.08 x 10^{-9}). Lower permeability was observed when examining transcellular transfer of thyroid hormones in B to A direction (mean $P_{app\ (B-A)}$ ± SD [cm/s], T_4: 2.08 x 10^{-6} ± 1.55 x 10^{-9}; T_3: 0.893 x 10^{-6} ± 2.51 x 10^{-9}). Similar results were obtained with T_4 and T_3 permeability after 60 minutes of incubation using the same system in A to B (mean $P_{app\ (A-B)}$ ± SD [cm/s]; T_4: 2.75 x 10^{-6} ± 0.57 x 10^{-6}; T_3: 3.36 x 10^{-6} ± 0.77 x 10^{-6}, data not shown) or B to A direction (mean $P_{app\ (A-B)}$ ± SD [cm/s]; T_4: 2.34 x 10^{-6} ± 0.32 x 10^{-6}; T_3: 1.74 x 10^{-6} ± 0.36 x 10^{-6}). However, calculating the uptake-ratio, which was conducted similar to the commonly used efflux-ratio, but dividing $P_{app\ (A-B)}$ by $P_{app\ (B-A)}$, revealed a factor of 1.779 ± 0.130 and 3.203 ± 0.909 for T_4 and T_3, respectively, highlighting that there is a component in cellular transfer that enhances A to B flux, despite that low permeability observed. Addition of atorvastatin [10 µM] as known inhibitor of OATP2B1 in the bi-directional permeability assessment,

Downloaded from molpharm.aspetjournals.org at ASPET Journals on April 18, 2024

Molecular Pharmacology Fast Forward. Published on May 7, 2018 as DOI: 10.1124/mol.117.111161
This article has not been copyedited and formatted. The final version may differ from this version.

significantly changed the uptake-ratio ($P_{app\,(A-B)}$/ $P_{app\,(B-A)}$) for T_4 and T_3 (Figure 6). These results indicate the presence of atorvastatin-sensitive, thyroid hormone transporters in Caco-2 cells.

Transcriptional regulation of OATP2B1 by thyroid hormones. Furthermore, we examined whether thyroxine (T_4, 100 nM) or triiodothyronine (T_3, 100 nM) treatment influences the expression of OATP2B1 variants in Caco-2 or Huh-7 cells. Both OATP2B1 1B and 1E variants are expressed in Caco-2 and Huh-7 cells (Knauer et al., 2013). We found that T_3 and T_4 treatments increased the mRNA expression of the intestinal OATP2B1 1B variant by 10-fold (mean % of DMSO control ± SEM, 1008 ± 240% of control, $p < 0.05$), and 4.8-fold (480 ± 140% of control, $p < 0.05$), respectively, in Caco-2 cells (Figure 7A). However, the thyroid hormones did not appreciably increase the OATP2B1 1B mRNA expression in Huh-7 cells (Figure 7D). The liver-enriched OATP2B1 1E variant mRNA expression was also induced 5.5-fold (549 ± 118% of control, $p < 0.05$) by T_3 and 2.7-fold (265 ± 69% of control, $p < 0.05$) by T_4 in Caco-2 cells (Figure 7B), but again not in Huh-7 cells (Figure 7E). For controls, we examined the expression of DIO1 and ABCB1 (P-glycoprotein, P-gp); two well-recognized thyroid hormone receptor target genes. As expected, both T_3 and T_4 treatments induced the expression of DIO1 in both Caco-2 (Figure 7C) and Huh-7 cells (Figure 7F). Induction was also observed for the expression of ABCB1 in Caco-2 (mean % of DMSO control ± SD, T_3: 9100 ± 8366%; T_4: 2054 ± 507.8 %; n=5, Kuskal-Wallis test, $p < 0.05$), and in Huh-7 cells (T_3: 148.2 ± 52.6 %; T_4: 161.1 ± 63.87 %; n=5, Kuskal-Wallis test, $p < 0.05$) (data not shown). Similar results were observed when testing the influence of thyroid hormones on OATP2B1 protein expression in differentiated Caco-2 cells cultivated for 14 days prior to thyroid hormone exposure. As shown in Figure 7G and 7H, expression of OATP2B1 was significantly increased by 2.6-fold in presence of T_3, and by 2.9-fold in presence of T_4. We additionally examined thyroid hormone-mediated regulation of OATP2B1 expression in other intestinal and liver cell lines. With intestinal LS180 cells, there was significant increment in

Downloaded from molpharm.aspetjournals.org at ASPET Journals on April 18, 2024

Molecular Pharmacology Fast Forward. Published on May 7, 2018 as DOI: 10.1124/mol.117.111161
This article has not been copyedited and formatted. The final version may differ from this version.

the OATP2B1 isoform 1E mRNA expression after exposure to T_3 (mean expression % of DMSO control ± SD; DMSO *vs.* T_3 *vs.* T_4; 117.92 ± 12.99 *vs.* 294.07 ± 41.46 *vs.* 244.36 ± 156.71; n=3 independent replicates each in triplicates; $p<0.05$; Kruskal-Wallis test with Dunn's multiple comparisons test). In LS180 cells, the amount of ABCB1 mRNA was also significantly increased by T_3 treatment (DMSO *vs.* T3 *vs.* T4; 121.93 ± 16.95 vs. 1286.14 ± 256.45 vs. 738.32 ± 400.22; $p<0.05$). However, for both genes we did not observe changes in expression after exposure of LS180 cells to T_4. It is notable that the mRNA expressions of the OATP2B1 1B variant and that of DIO1 were not detected in LS180 cells. In HepG2 cells we tested the influence of T_3 on DIO1, ABCB1, and the OATP2B1 variants, and observed no significant change in mRNA expression of any gene (mean expression % of DMSO control ± SD; DMSO *vs.* T_3 DIO1: 105.01 ± 2.81 *vs.* 155.71 ± 19.93; ABCB1: 105.99 ± 2.48 *vs.* 89.96 ± 15.25; OATP2B1 1E: 103.81 ± 1.64 *vs.* 144.9 ± 10.11; OATP2B1 1B 104.81 ± 2.22 *vs.* 139.92 ± 5.60; n=3 independent replicates each in triplicates; $p>0.05$ n=3 independent replicates each in triplicates Mann-Whitney test). Taken together, these results demonstrate that thyroid hormones are positive regulators of the OATP2B1 gene expression in a cell type-dependent manner.

OATP2B1 promoter analysis and cell-based reporter gene assays. Transcriptional regulation by thyroid hormones is mediated by TRs. These nuclear receptors bind to DNA response elements in the promoter region of their target genes. We performed an *in silico* analysis to search for the TR DNA-bindings motifs DR4, ER6, or DR1 in the *SLCO2B1* 1b or *SLCO2B1* 1e promoters (Knauer et al., 2013). As summarized in Table 2 and shown in Figure 8A, multiple potential response elements for TRs were identified in the sequences analyzed. In detail, the ER6 motif (AGTCCTcagtccAGGAAA) in position -899 to-882 exhibited highest rank in the analysis of the *SLCO2B1* 1b promoter sequence, while the previously reported DR1 motif (AGGGCAaAGTCCA in position -17 to -4), had the highest score in the *SLCO2B1* 1e promoter. Considering the

Downloaded from molpharm.aspetjournals.org at ASPET Journals on April 18, 2024

Molecular Pharmacology Fast Forward. Published on May 7, 2018 as DOI: 10.1124/mol.117.111161
This article has not been copyedited and formatted. The final version may differ from this version.

differential tissue/cell expression of TRα and cell-type specific induction of OATP2B1 by thyroid hormones, we examined whether the SLCO2B1 1b and SLCO2B1 1 e promoters were activated in presence of TRα and its activating ligand T_3 in cell-based luciferase assays. The TR-sensitive DIO1-promoter served as control in these experiments. We observed significantly enhanced luciferase activity after treatment with T_3 in HeLa cells transfected with the *SLCO2B1* 1b promoter (mean luciferase activity fold of pGL3b control ± SD; DMSO *vs.* T_3; 1.364 ± 0.141 *vs.* 2.268 ± 0.444; $p<0.05$ student's t-test, Figure 8B). Similarly, T_3 treatment enhanced the *SLCO2B1* 1e promoter luciferase activity (1.197 ± 0.142 *vs.* 2.260 ± 0.485; $p<0.05$ student's t-test, Figure 8C). These results demonstrate that both SLCO2B1 1b and SLCO2B1 1e promoters are transactivated by TRα.

Discussion

We report interaction of thyroid hormones with the function and expression of OATP2B1. This ubiquitously expressed transporter, with suspected function in the intestinal absorption of drugs, was inhibited by all thyroid hormone (TH) derivatives tested in OATP2B1-expressing cells. Furthermore, counter-flow experiments assessing the influence of TH-derivatives on the cellular equilibrium of E_1S at steady-state suggested, that T_3, T_4 and rT_3 are not only inhibitors, but also substrates of OATP2B1. This notion was further supported by findings showing that the presence of OATP2B1 significantly enhanced intracellular TH signaling as observed in cell-based reporter gene assays comparing MDCKII and MDCKII-OATP2B1 cells. The presence of an active transport component in the transcellular transport of triiodothyronine and thyroxine was supported by results of transcellular flux experiments in the intestinal cell line Caco-2. Indeed, we observed enhanced permeability in A to B direction for both thyroxine and triiodothyronine, resulting in an uptake-ratio ($P_{app\ (A-B)}$ / $P_{app\ (B-A)}$) of about 1.8 and about 3.2 for T_4 and T_3, respectively. Atorvastatin, which is a known substrate and competitive inhibitor of OATP2B1 (Grube et al.,

Downloaded from molpharm.aspetjournals.org at ASPET Journals on April 18, 2024

Molecular Pharmacology Fast Forward. Published on May 7, 2018 as DOI: 10.1124/mol.117.111161
This article has not been copyedited and formatted. The final version may differ from this version.

2006), significantly reduced this ratio for triiodothyronine and thyroxine. The observed reduction in TH uptake ratio by atorvastatin could certainly be interpreted in terms of reduced uptake mediated by apically localized OATP2B1, but it should also be noted that multiple transporters are expressed in enterocytes and Caco-2 cells, of relevance being the efflux transporter ABCB1 (P-gp) which has previously been reported to also transport triiodothyronine (Mitchell et al., 2005). Moreover, atorvastatin is not a specific OATP2B1 inhibitor, and thus also interacts with several efflux transporters including aforementioned ABCB1 (Chen et al., 2005). Despite that, we observed reduction in net absorption of thyroid hormones in presence of atorvastatin in Caco-2 cells, even if it is likely that there has been reduced apical thyroid hormone efflux by ABCB1 in presence of atorvastatin.

As mentioned before, localization of OATP2B1 in enterocytes is matter of an ongoing debate, which was sparked by recent experiments by Kaiser *et al.* indicating that OATP2B1 is localized in the basolateral membrane of enterocytes (Keiser et al., 2017). This localization would be expected to result in an increase of the uptake-ratio of OATP2B1 substrates in presence of an inhibitor specific to this transporter, which has not been observed in the herein reported experiments. Even if we are not able to dissect the contribution of each Caco-2 transporter to thyroid hormone fluxes as atorvastatin is a potent inhibitor of OATP2B1, but not specific for this transporter, our observation, which showed a reduction in the ratio, would be in agreement with findings by others showing expression of OATP2B1 in the apical membrane of enterocytes and Caco-2 cells (Kobayashi et al., 2003; Tamai et al., 2001).

Our data demonstrated inhibition of OATP2B1 function by triiodothyronine and thyroxine with *in vitro* IC_{50} values in the micromolar range. Whether this inhibition is of clinical relevance with respect to thyroid hormone being a perpetrator of pharmacokinetic drug interactions especially in

Downloaded from molpharm.aspetjournals.org at ASPET Journals on April 18, 2024

Molecular Pharmacology Fast Forward. Published on May 7, 2018 as DOI: 10.1124/mol.117.111161
This article has not been copyedited and formatted. The final version may differ from this version.

other tissues than intestine is uncertain. However, normal thyroxine plasma concentrations range from 0.59-1.54 μM. Furthermore, thyroxine is significantly bound to serum proteins resulting in free T_4 concentrations of 0.09 to 0.24 nM. Considering these low physiological free plasma concentrations, it seems unlikely that thyroxine would alter the tissue distribution/elimination of drugs through inhibition of OATP2B1. Similar considerations could be taken for triiodothyronine whose physiological plasma total concentrations range from 0.01 to 0.03 μM.

At the clinical level, little is known regarding the role of OATP2B1 in the intestinal absorption of levothyroxine. A clinical study was conducted by Lilja *et al.*, motivated by a case in which a patient experienced significant changes in levothyroxine efficacy after grapefruit juice ingestion (Lilja et al., 2005). Grapefruit juice is known to inhibit intestinal OATP2B1 (Satoh et al., 2005). The investigators found that grapefruit juice slightly reduced levothyroxine $AUC_{0\text{-}6h}$ by 9%, which was concluded to be clinically insignificant. While this finding argues against the role of OATP2B1 in the oral absorption of levothyroxine, it is notable that inhibition of OATP2B1 by grapefruit juice may be drug-specific as the transporter possesses two binding sites for substrates and inhibitors (Shirasaka et al., 2014; Shirasaka et al., 2012). Characterization of levothyroxine binding to the high and low affinity binding site and modulation by grapefruit juice remains to be determined. Another explanation for the lack of a significant pharmacokinetic interaction in the aforementioned study may be that it was conducted in healthy volunteers while the clinical case report was in a patient with hypothyroidism. The possibility that hypothyroidism may influence the magnitude of the juice-levothyroxine interaction is supported by our finding that OATP2B1 expression is regulated by thyroid hormones.

We showed up-regulation of OATP2B1 mRNA and protein expression in Caco-2 cells by thyroid hormones, suggesting that thyroid hormone status influences expression and activity of the

Downloaded from molpharm.aspetjournals.org at ASPET Journals on April 18, 2024

Molecular Pharmacology Fast Forward. Published on May 7, 2018 as DOI: 10.1124/mol.117.111161
This article has not been copyedited and formatted. The final version may differ from this version.

intestinal uptake transporter. A similar transcriptional regulation was observed when assessed in LS180 cells, an additional intestinal cell model previously used to show induction of ABCB1 after exposure to thyroid hormones (Mitin et al., 2004). Interestingly, when examined in Huh-7 and HepG2 cells, ~~a~~ models for hepatocytes, thyroid hormones did not affect OATP2B1 expression, pointing to a cell model specific regulation. Expression of the thyroid hormone receptor TRβ was observed in all cell models used in our study, suggesting that differential expression of this receptor is not the reason underlying the cell-specific effect. In contrast, quantification of TRα revealed a lower amount of this nuclear receptor in hepatic cell models, suggesting that this nuclear receptor may be involved in the regulation of OATP2B1 expression observed in the intestinal cells. Two N-terminal protein variants of OATP2B1 (variants 1B and 1E) have been described, these variants are assumed to be transcriptionally regulated by different promoter regions as their transcriptional start sites differ. In accordance are findings showing that the liver enriched *SLCO2B1* 1E, but not the ubiquitously expressed *SLCO2B1* 1B transcriptional start site variant is regulated by the transcription factor HNF4α (Knauer et al., 2013). However, with respect to regulation by TRα we observed significant transactivation of both *SLCO2B1* promoters. Considering that multiple potential binding sites for TRs were predicted in the promoter sequences of *SLCO2B1*-1b and *SLCO2B1*-1e and that TRα is the predominant nuclear receptor in intestine (Sirakov and Plateroti, 2011), differences in TRα expression levels may be the mechanism underlying the observed differences in transcriptional regulation in hepatic (Huh-7, HepG2) and intestinal (Caco-2, LS180) cells.

There is evidence that thyroid hormone status modulates expression and function of other drug transporters in the intestinal wall. For example, the efflux transporter ABCB1 that limits intestinal drug absorption is regulated by thyroid hormones (Mitin et al., 2004). Indeed, the required doses of the ABCB1 substrate digoxin, used to treat cardiac failure and to control heart rate, differs among

Downloaded from molpharm.aspetjournals.org at ASPET Journals on April 18, 2024

Molecular Pharmacology Fast Forward. Published on May 7, 2018 as DOI: 10.1124/mol.117.111161
This article has not been copyedited and formatted. The final version may differ from this version.

patients suffering from hyper- or hypothyroidism compared to patients with normal thyroid function. Specifically, higher and lower digoxin maintenance doses are needed with hyperthyroidism and hypothyroidism, respectively (Burk et al., 2010). It is notable that digoxin is not a substrate of OATP2B1 (Taub et al., 2011). Another study by Jin *et al.* showed that the trough plasma concentrations of the ABCB1 substrate, cyclosporin A, were lower in patients taking levothyroxine. Increased expression of abcb1a/abcb1b in mice after long-term treatment with levothyroxine was found to explain this clinical drug-drug interaction (Jin et al., 2005). Lastly, Siegmund *et al.* reported induction of intestinal ABCB1 in humans treated with L-thyroxine. However, this induction of ABCB1 resulted only in minor, non-clinically relevant changes in the pharmacokinetics of talinolol, an ABCB1 substrate (Siegmund et al., 2002). It is interesting that talinolol is also a substrate of the uptake transporters OATP2B1 and OATP1A2 (Shirasaka et al., 2010), despite that it is not anionic. It is possible that thyroid hormone-mediated upregulation of the intestinal efflux mechanisms could be counteracted by the concomitant upregulation of OATP2B1, leading to minimal pharmacokinetic consequences for talinolol.

In conclusion, we report that T_3 and T_4 are substrates of OATP2B1, indicating a novel mechanism for regulation of thyroid hormone homeostasis by influencing hormone distribution and absorption during replacement therapy. In addition, we showed up-regulation of OATP2B1 by thyroid hormones, which may be of relevance for intestinal absorption of substrate drugs with narrow therapeutic index.

Downloaded from molpharm.aspetjournals.org at ASPET Journals on April 18, 2024

Molecular Pharmacology Fast Forward. Published on May 7, 2018 as DOI: 10.1124/mol.117.111161
This article has not been copyedited and formatted. The final version may differ from this version.

Acknowledgment

We want to thank Janine Hussner for the support during manuscript preparation.

Authorship Contributions:

Participated in research design: Ferreira, Meyer zu Schwabedissen, Oufir, Schäfer, Tirona

Conducted experiments: Ferreira, Meyer zu Schwabedissen, Oufir, Schäfer, Seibert, Tirona

Contributed analytical tools: Hamburger, Meyer zu Schwabedissen, Tirona

Performed data analysis: Ferreira, Meyer zu Schwabedissen, Oufir, Schäfer, Tirona

Wrote and contributed to the writing of the manuscript: Ferreira, Hamburger, Meyer zu Schwabedissen, Oufir, Schäfer, Tirona

Downloaded from molpharm.aspetjournals.org at ASPET Journals on April 18, 2024

Molecular Pharmacology Fast Forward. Published on May 7, 2018 as DOI: 10.1124/mol.117.111161
This article has not been copyedited and formatted. The final version may differ from this version.

References

Ayers S, Switnicki MP, Angajala A, Lammel J, Arumanayagam AS and Webb P (2014) Genome-wide binding patterns of thyroid hormone receptor beta. *PLoS One* **9**(2): e81186.

Bernal J, Guadano-Ferraz A and Morte B (2015) Thyroid hormone transporters--functions and clinical implications. *Nat Rev Endocrinol* **11**(7): 406-417.

Burk O, Brenner SS, Hofmann U, Tegude H, Igel S, Schwab M, Eichelbaum M and Alscher MD (2010) The impact of thyroid disease on the regulation, expression, and function of ABCB1 (MDR1/P glycoprotein) and consequences for the disposition of digoxin. *Clin Pharmacol Ther* **88**(5): 685-694.

Centanni M, Gargano L, Canettieri G, Viceconti N, Franchi A, Delle Fave G and Annibale B (2006) Thyroxine in goiter, Helicobacter pylori infection, and chronic gastritis. *N Engl J Med* **354**(17): 1787-1795.

Chen C, Mireles RJ, Campbell SD, Lin J, Mills JB, Xu JJ and Smolarek TA (2005) Differential interaction of 3-hydroxy-3-methylglutaryl-coa reductase inhibitors with ABCB1, ABCC2, and OATP1B1. *Drug Metab Dispos* **33**(4): 537-546.

Drozdzik M, Groer C, Penski J, Lapczuk J, Ostrowski M, Lai Y, Prasad B, Unadkat JD, Siegmund W and Oswald S (2014) Protein abundance of clinically relevant multidrug transporters along the entire length of the human intestine. *Mol Pharm* **11**(10): 3547-3555.

Fujiwara K, Adachi H, Nishio T, Unno M, Tokui T, Okabe M, Onogawa T, Suzuki T, Asano N, Tanemoto M, Seki M, Shiiba K, Suzuki M, Kondo Y, Nunoki K, Shimosegawa T, Iinuma K, Ito S, Matsuno S and Abe T (2001) Identification of thyroid hormone transporters in humans: different molecules are involved in a tissue-specific manner. *Endocrinology* **142**(5): 2005-2012.

Garmendia Madariaga A, Santos Palacios S, Guillen-Grima F and Galofre JC (2014) The incidence and prevalence of thyroid dysfunction in Europe: a meta-analysis. *J Clin Endocrinol Metab* **99**(3): 923-931.

Glaeser H, Bailey DG, Dresser GK, Gregor JC, Schwarz UI, McGrath JS, Jolicoeur E, Lee W, Leake BF, Tirona RG and Kim RB (2007) Intestinal drug transporter expression and the impact of grapefruit juice in humans. *Clin Pharmacol Ther* **81**(3): 362-370.

Goldberg AS, Tirona RG, Asher LJ, Kim RB and Van Uum SH (2013) Ciprofloxacin and rifampin have opposite effects on levothyroxine absorption. *Thyroid* **23**(11): 1374-1378.

Grube M, Köck K, Oswald S, Draber K, Meissner K, Eckel L, Bohm M, Felix SB, Vogelgesang S, Jedlitschky G, Siegmund W, Warzok R and Kroemer HK (2006) Organic anion transporting polypeptide 2B1 is a high-affinity transporter for atorvastatin and is expressed in the human heart. *Clin Pharmacol Ther* **80**(6): 607-620.

Harper JN and Wright SH (2013) Multiple mechanisms of ligand interaction with the human organic cation transporter, OCT2. *Am J Physiol Renal Physiol* **304**(1): F56-67.

Hollowell JG, Staehling NW, Flanders WD, Hannon WH, Gunter EW, Spencer CA and Braverman LE (2002) Serum TSH, T(4), and thyroid antibodies in the United States population (1988 to 1994): National Health and Nutrition Examination Survey (NHANES III). *J Clin Endocrinol Metab* **87**(2): 489-499.

Hubatsch I, Ragnarsson EG and Artursson P (2007) Determination of drug permeability and prediction of drug absorption in Caco-2 monolayers. *Nat Protoc* **2**(9): 2111-2119.

Ianiro G, Mangiola F, Di Rienzo TA, Bibbo S, Franceschi F, Greco AV and Gasbarrini A (2014) Levothyroxine absorption in health and disease, and new therapeutic perspectives. *Eur Rev Med Pharmacol Sci* **18**(4): 451-456.

Irving SA, Vadiveloo T and Leese GP (2015) Drugs that interact with levothyroxine: an observational study from the Thyroid Epidemiology, Audit and Research Study (TEARS). *Clin Endocrinol (Oxf)* **82**(1): 136-141.

Downloaded from molpharm.aspetjournals.org at ASPET Journals on April 18, 2024

Molecular Pharmacology Fast Forward. Published on May 7, 2018 as DOI: 10.1124/mol.117.111161
This article has not been copyedited and formatted. The final version may differ from this version.

Jin M, Shimada T, Shintani M, Yokogawa K, Nomura M and Miyamoto K (2005) Long-term levothyroxine treatment decreases the oral bioavailability of cyclosporin A by inducing P-glycoprotein in small intestine. *Drug Metab Pharmacokinet* **20**(5): 324-330.

Keiser M, Kaltheuner L, Wildberg C, Muller J, Grube M, Partecke LI, Heidecke CD and Oswald S (2017) The Organic Anion-Transporting Peptide 2B1 Is Localized in the Basolateral Membrane of the Human Jejunum and Caco-2 Monolayers. *J Pharm Sci*.

Knauer MJ, Girdwood AJ, Kim RB and Tirona RG (2013) Transport function and transcriptional regulation of a liver-enriched human organic anion transporting polypeptide 2B1 transcriptional start site variant. *Molecular pharmacology* **83**(6): 1218-1228.

Kobayashi D, Nozawa T, Imai K, Nezu J, Tsuji A and Tamai I (2003) Involvement of human organic anion transporting polypeptide OATP-B (SLC21A9) in pH-dependent transport across intestinal apical membrane. *J Pharmacol Exp Ther* **306**(2): 703-708.

Koenen A, Kroemer HK, Grube M and Meyer zu Schwabedissen HE (2011) Current understanding of hepatic and intestinal OATP-mediated drug-drug interactions. *Expert Rev Clin Pharmacol* **4**(6): 729-742.

Kohrle J (2007) Thyroid hormone transporters in health and disease: advances in thyroid hormone deiodination. *Best Pract Res Clin Endocrinol Metab* **21**(2): 173-191.

Kullak-Ublick GA, Ismair MG, Stieger B, Landmann L, Huber R, Pizzagalli F, Fattinger K, Meier PJ and Hagenbuch B (2001) Organic anion-transporting polypeptide B (OATP-B) and its functional comparison with three other OATPs of human liver. *Gastroenterology* **120**(2): 525-533.

Lee W, Glaeser H, Smith LH, Roberts RL, Moeckel GW, Gervasini G, Leake BF and Kim RB (2005) Polymorphisms in human organic anion-transporting polypeptide 1A2 (OATP1A2): implications for altered drug disposition and central nervous system drug entry. *J Biol Chem* **280**(10): 9610-9617.

Leuthold S, Hagenbuch B, Mohebbi N, Wagner CA, Meier PJ and Stieger B (2009) Mechanisms of pH-gradient driven transport mediated by organic anion polypeptide transporters. *Am J Physiol Cell Physiol* **296**(3): C570-582.

Lilja JJ, Laitinen K and Neuvonen PJ (2005) Effects of grapefruit juice on the absorption of levothyroxine. *Br J Clin Pharmacol* **60**(3): 337-341.

Mitchell AM, Tom M and Mortimer RH (2005) Thyroid hormone export from cells: contribution of P-glycoprotein. *J Endocrinol* **185**(1): 93-98.

Mitin T, Von Moltke LL, Court MH and Greenblatt DJ (2004) Levothyroxine up-regulates P-glycoprotein independent of the pregnane X receptor. *Drug Metab Dispos* **32**(8): 779-782.

Mondal S, Raja K, Schweizer U and Mugesh G (2016) Chemistry and Biology in the Biosynthesis and Action of Thyroid Hormones. *Angew Chem Int Ed Engl* **55**(27): 7606-7630.

Pizzagalli F, Hagenbuch B, Stieger B, Klenk U, Folkers G and Meier PJ (2002) Identification of a novel human organic anion transporting polypeptide as a high affinity thyroxine transporter. *Mol Endocrinol* **16**(10): 2283-2296.

Podvinec M, Kaufmann MR, Handschin C and Meyer UA (2002) NUBIScan, an in silico approach for prediction of nuclear receptor response elements. *Mol Endocrinol* **16**(6): 1269-1279.

Pomari E, Nardi A, Fiore C, Celeghin A, Colombo L and Dalla Valle L (2009) Transcriptional control of human organic anion transporting polypeptide 2B1 gene. *J Steroid Biochem Mol Biol* **115**(3-5): 146-152.

Riley RJ, Foley SA, Barton P, Soars MG and Williamson B (2016) Hepatic drug transporters: the journey so far. *Expert Opin Drug Metab Toxicol* **12**(2): 201-216.

Satoh H, Yamashita F, Tsujimoto M, Murakami H, Koyabu N, Ohtani H and Sawada Y (2005) Citrus juices inhibit the function of human organic anion-transporting polypeptide OATP-B. *Drug Metab Dispos* **33**(4): 518-523.

Shirasaka Y, Kuraoka E, Spahn-Langguth H, Nakanishi T, Langguth P and Tamai I (2010) Species difference in the effect of grapefruit juice on intestinal absorption of talinolol between human and rat. *J Pharmacol Exp Ther* **332**(1): 181-189.

Downloaded from molpharm.aspetjournals.org at ASPET Journals on April 18, 2024

Molecular Pharmacology Fast Forward. Published on May 7, 2018 as DOI: 10.1124/mol.117.111161
This article has not been copyedited and formatted. The final version may differ from this version.

Shirasaka Y, Mori T, Murata Y, Nakanishi T and Tamai I (2014) Substrate- and dose-dependent drug interactions with grapefruit juice caused by multiple binding sites on OATP2B1. *Pharm Res* **31**(8): 2035-2043.

Shirasaka Y, Mori T, Shichiri M, Nakanishi T and Tamai I (2012) Functional pleiotropy of organic anion transporting polypeptide OATP2B1 due to multiple binding sites. *Drug Metab Pharmacokinet* **27**(3): 360-364.

Siegmund W, Altmannsberger S, Paneitz A, Hecker U, Zschiesche M, Franke G, Meng W, Warzok R, Schroeder E, Sperker B, Terhaag B, Cascorbi I and Kroemer HK (2002) Effect of levothyroxine administration on intestinal P-glycoprotein expression: consequences for drug disposition. *Clin Pharmacol Ther* **72**(3): 256-264.

Sirakov M and Plateroti M (2011) The thyroid hormones and their nuclear receptors in the gut: from developmental biology to cancer. *Biochim Biophys Acta* **1812**(8): 938-946.

Sugiyama D, Kusuhara H, Taniguchi H, Ishikawa S, Nozaki Y, Aburatani H and Sugiyama Y (2003) Functional characterization of rat brain-specific organic anion transporter (Oatp14) at the blood-brain barrier: high affinity transporter for thyroxine. *J Biol Chem* **278**(44): 43489-43495.

Tamai I, Nezu J, Uchino H, Sai Y, Oku A, Shimane M and Tsuji A (2000) Molecular identification and characterization of novel members of the human organic anion transporter (OATP) family. *Biochem Biophys Res Commun* **273**(1): 251-260.

Tamai I, Nozawa T, Koshida M, Nezu J, Sai Y and Tsuji A (2001) Functional characterization of human organic anion transporting polypeptide B (OATP-B) in comparison with liver-specific OATP-C. *Pharm Res* **18**(9): 1262-1269.

Taub ME, Mease K, Sane RS, Watson CA, Chen L, Ellens H, Hirakawa B, Reyner EL, Jani M and Lee CA (2011) Digoxin is not a substrate for organic anion-transporting polypeptide transporters OATP1A2, OATP1B1, OATP1B3, and OATP2B1 but is a substrate for a sodium-dependent transporter expressed in HEK293 cells. *Drug Metab Dispos* **39**(11): 2093-2102.

van der Deure WM, Friesema EC, de Jong FJ, de Rijke YB, de Jong FH, Uitterlinden AG, Breteler MM, Peeters RP and Visser TJ (2008) Organic anion transporter 1B1: an important factor in hepatic thyroid hormone and estrogen transport and metabolism. *Endocrinology* **149**(9): 4695-4701.

van der Deure WM, Peeters RP and Visser TJ (2010) Molecular aspects of thyroid hormone transporters, including MCT8, MCT10, and OATPs, and the effects of genetic variation in these transporters. *J Mol Endocrinol* **44**(1): 1-11.

Visser WE, Friesema EC and Visser TJ (2011) Minireview: thyroid hormone transporters: the knowns and the unknowns. *Mol Endocrinol* **25**(1): 1-14.

Downloaded from molpharm.aspetjournals.org at ASPET Journals on April 18, 2024

Molecular Pharmacology Fast Forward. Published on May 7, 2018 as DOI: 10.1124/mol.117.111161
This article has not been copyedited and formatted. The final version may differ from this version.

Footnotes

The work was supported by the Swiss National Foundation [Grant: 31003A_149603] awarded to Henriette Meyer zu Schwabedissen and the Canadian Institutes of Health Research [Grant: MOP-136909] awarded to Rommel Tirona. The herein reported study is part of the master thesis of Anima Schäfer and part of the PhD thesis of Celio Ferreira.

Downloaded from molpharm.aspetjournals.org at ASPET Journals on April 18, 2024

Molecular Pharmacology Fast Forward. Published on May 7, 2018 as DOI: 10.1124/mol.117.111161
This article has not been copyedited and formatted. The final version may differ from this version.

Figure Legends

Figure 1: Validation of OATP2B1 expression and function in stably transfected MDCKII cells. Immunofluorescent staining of MDCKII-OATP2B1 and MDCKII cells revealed localization of the transporter in the basolateral membrane of polarized MDCKII cells overexpressing the transporter. No signal was observed in MDCKII cells (A). Immunoblot analysis verified high expression comparing MDCKII and MDCKII-OATP2B1 cells as shown in a representative blot (B). Uptake of [^{3}H]-estrone 3-sulfate was significantly enhanced in presence of the transporter, while reduced by co-incubation with atorvastatin (C).

Figure 2: Inhibition of OATP2B1 mediated uptake by thyroid hormone derivatives. Uptake of [^{3}H]-estrone 3-sulfate [E_1S] in MDCKII-OATP2B1 was determined in presence of different thyroid hormones derived from thyroxine (A). Cellular accumulation of E_1S was determined after incubation with increasing concentrations of thyroxine (T_4, B), triiodothyronine (T_3, C), reverse triiodothyronine (rT_3, D), or thyroxine 4-O-β D glucuronide (T_4G, E). The logarithmic inhibitor response curves were fitted to determine IC_{50} and the respective confidence intervals (CI). The data presented are of n=3 independent replicates each in triplicates.

Figure 3. Competitive Counter-flow assays in MDCKII-OATP2B1 cells. Assessment of time-dependent accumulation of [^{3}H]-estrone-3-sulfate (E_1S) comparing MDCKII and MDCKII-OATP2B1 cells (A). Counter-flow experiments were conducted after reaching the steady-state of E_1S at 30 min of incubation. The cellular amount of the radiotracer was determined after 1 min incubation with 50 µM E_1S, 30 µM atorvastatin, 1 mM camptothecin, 25 µM T_4, 10 µM T_3, 1 mM rT_3 or 400 µM T_4G. The detected amount of radiotracer was normalized to that in cells treated with solvent control. Data are presented as mean ± SD (n=3 independent replicates each in triplicates).

Downloaded from molpharm.aspetjournals.org at ASPET Journals on April 18, 2024

Molecular Pharmacology Fast Forward. Published on May 7, 2018 as DOI: 10.1124/mol.117.111161
This article has not been copyedited and formatted. The final version may differ from this version.

For the statistical analysis, one-way ANOVA with Dunnett's multiple comparisons test was used (*$p \leq 0.05$).

Figure 4: Influence of OATP2B1 expression on transactivation of the DIO1-promoter. Transactivation of the DIO1-promoter was determined by cell based dual luciferase assays comparing MDCKII with MDCKII-OATP2B1 cells (see insert). Luciferase activity was assessed after treatment with triiodothyronine (T_3) or thyroxine (T_4). MDCKII or MDCKII-OATP2B1 cells were transfected with DIO1-pGL3basic, and eukaryotic expression vectors encoding for TRβ (A), RXRα (B) or both (C). Data are presented as mean ± SD (n=3 independent replicates each in triplicates). For the statistical analysis, the two-way ANOVA with Sidak's multiple comparisons test was used (*$p \leq 0.05$).

Figure 5: Gene expression analysis in tissues and commonly used cellular models. Expression of the thyroid hormone receptor α (TR α) and the thyroid hormone receptor β (TRβ) was quantified by real-time PCR in different human tissues (A,B) and corresponding cellular models (C,D) using specific TaqMan® gene expression assays. In addition, mRNA amount of two isoforms of the Organic Anion Transporting Polypeptide 2B1 (OATP2B1) was assessed. Both isoform 1B and isoform 1E (*SLCO2B1* 1B and 1E) were quantified with SYBRgreen assays. Relative expression of each gene was calculated according to the ΔΔCt method. Data are presented mean ± SD, n=3 independent replicates each in triplicates.

Figure 6: Transcellular flux of thyroid hormones and localization of OATP2B1 in cultured Caco-2 cells. Caco-2 cells cultivated for 14 days in a Transwell® system were used to assess apical to basolateral (A-B) or basolateral to apical (B-A) flux of thyroxine (T_4), or triiodothyronine (T_3) in presence of solvent control (DMSO), or atorvastatin (10 μM). The unidirectional apparent permeability coefficients (P_{app}) for T_4 (B) and T_3 (D) were used to calculate the uptake-ratio (P_{app}

Downloaded from molpharm.aspetjournals.org at ASPET Journals on April 18, 2024

Molecular Pharmacology Fast Forward. Published on May 7, 2018 as DOI: 10.1124/mol.117.111161
This article has not been copyedited and formatted. The final version may differ from this version.

(A-B)/P_{app} (B-A)) for T_4 (A) and T_3 (C). Data are presented as mean ± SD (n = 3 independent replicates). For statistical analysis, the Sidak's multiple comparison test was used (*$p \leq 0.05$).

Figure 7: Influence of thyroid hormones on expression of OATP2B1. Expression of *SLCO2B1* isoform 1B (A) *SLCO2B1* isoform 1E (B) and deiodinase type 1 (C) mRNA was quantified by real-time PCR after 48 hours of treatment of differentiated Caco-2 cells with triiodothyronine (T_3, 100 nM) or L-thyroxine (T_4, 100 nM). Amount of *SLCO2B1* isoform 1B (D) *SLCO2B1* isoform 1E (E) and deiodinase type 1 (F) mRNA was quantified by real-time PCR in Huh-7 cells treated with T_3 (100 nM) or T_4 (100 nM). Expression data were calculated by the ΔΔ-Ct method where expression was related to that of a housekeeping gene and then normalized to the solvent control. Data are presented as mean ± SEM of n=5 experiments. Gene expression was analyzed with a Kruskal Wallis-test with Dunn's multiple comparisons test. OATP2B1 protein expression was assessed by Western blot analysis (representative result, G). Actin served as loading control. Data obtained by densitometry of n=3 experiments are presented as mean ± SD, and comparisons were analyzed by one-way ANOVA with Dunnett's multiple comparisons test (E) (* $p < 0.05$).

Figure 8: Thyroid hormone receptor α (TRα) mediated transactivation of the SLCO2B1-1b or SLCO2B1-1e promoter. Arrangement of the respective region of the *SLCO2B1* gene locus depicting the different exons 1a to 1e. For the transcriptional start site variants SLCO2B1-1B and 1E details on the localization of potential TRREs in the respective promoter region are shown (A). Cell based reporter gene assays were performed in HeLa cells transiently transfected with the SLCO2B1-1b (B), SLCO2B1-1e (C), or the Dio1 (D)-promoter and treated with triiodothyronine (T3; 10μM) or solvent control. Data are shown as mean luciferase activity fold of pGL3-basic (n=3 independent replicates each in triplicates). *<0.05 student's t-test.

Downloaded from molpharm.aspetjournals.org at ASPET Journals on April 18, 2024

Molecular Pharmacology Fast Forward. Published on May 7, 2018 as DOI: 10.1124/mol.117.111161
This article has not been copyedited and formatted. The final version may differ from this version.

Tables

Table 1: Optimized MS/MS parameters in ESI positive mode for analytes and the corresponding internal standards (I.S.).

Analyte **I.S.**	**MRM transitions**	**Cone voltage** [V]	**Collision energy** [eV]
T_3	651.6→197.1	55	80
I.S. $^{13}C_6$ T_3	658.0→612.0	50	32
T_4	777.3→633.8	60	42
I.S. $^{13}C_6$ T_4	783.4→737.7	55	32

Downloaded from molpharm.aspetjournals.org at ASPET Journals on April 18, 2024

Molecular Pharmacology Fast Forward. Published on May 7, 2018 as DOI: 10.1124/mol.117.111161
This article has not been copyedited and formatted. The final version may differ from this version.

Table 2: Summary of potential thyroid hormone receptor (TR) response elements in the SLCO2B1 1b and SLCO2B1 1e promoter region. Analysis was performed using the publically available NUBIscan software. Response element marked with † exhibited highest score in the *in silico analysis* for this particular motif. Response element highlighted in bold had the highest score in the analysis of the respective promoter fragment. * Response element previously reported to be the most likely HNF4α binding site, resulting in constitutive activity of the promoter in cells, where this transcription factor is present (Knauer et al., 2013).

motif	sequence	position
SLCO2B1-1b promoter		
DR4-III†	GGGTCTgatcAGGTCA	-1756 to -1741
DR4-II	AGGACAgagaAGCCAA	-1078 to -1063
ER6-II	TATCCTgggtggAGGGAA	-1362 to -1345
ER6-I†	**AGTCCTcagtccAGGAAA**	**-899 to -882**
DR4-I	AGGCTGgaaaAGGACA	-405 to -390
SLCO2B1-1e promoter		
DR4-IV†	AGCACAtctgAGGCAA	-2170 to -2186
DR1-V	AGAGCAaGGGCCA	-2136 to -2149
ER6-I	TGACCTatttcaGGGTGA	-1241 to -1223
DR4-III	AGGTGGgagaAGGTCA	-1222 to -1206
DR1-IV	AGGTCTgAGGCCT	-996 to 983
DR1-III	AGGACAgATCTCA	-954 to -941
DR1-II	AGCCCAcAGGAAA	-167 to -155
DR4-II	AGGGAAgcacTGGCC	-55 to -40
DR4-1	TGGGCAggggAGGGAA	-46 to -30
DR1-I†*	**AGGGCAaAGTCCA**	**-17 to -4**

Downloaded from molpharm.aspetjournals.org at ASPET Journals on April 18, 2024

Molecular Pharmacology Fast Forward. Published on May 7, 2018 as DOI: 10.1124/mol.117.111161
This article has not been copyedited and formatted. The final version may differ from this version.

Figure 1

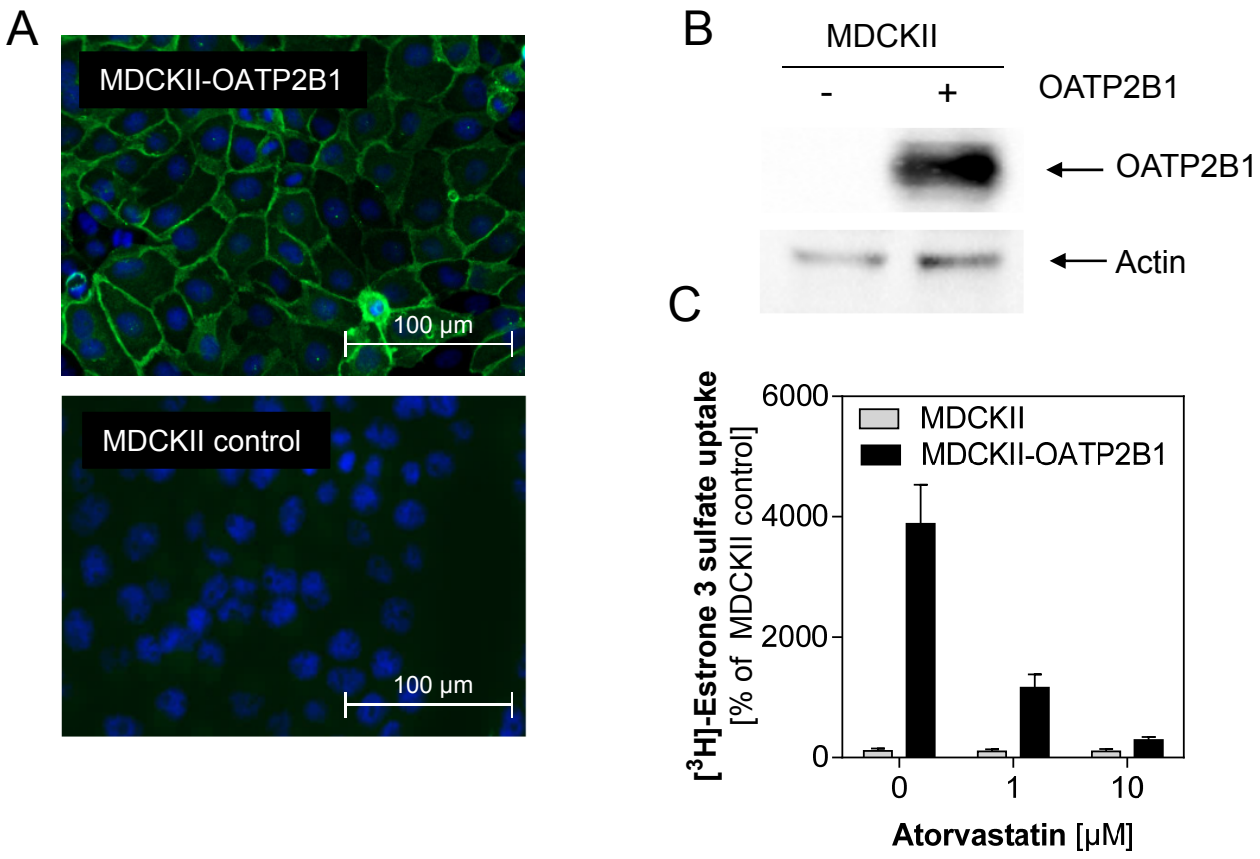

Downloaded from molpharm.aspetjournals.org at ASPET Journals on April 18, 2024

Molecular Pharmacology Fast Forward. Published on May 7, 2018 as DOI: 10.1124/mol.117.111161
This article has not been copyedited and formatted. The final version may differ from this version.

Figure 2

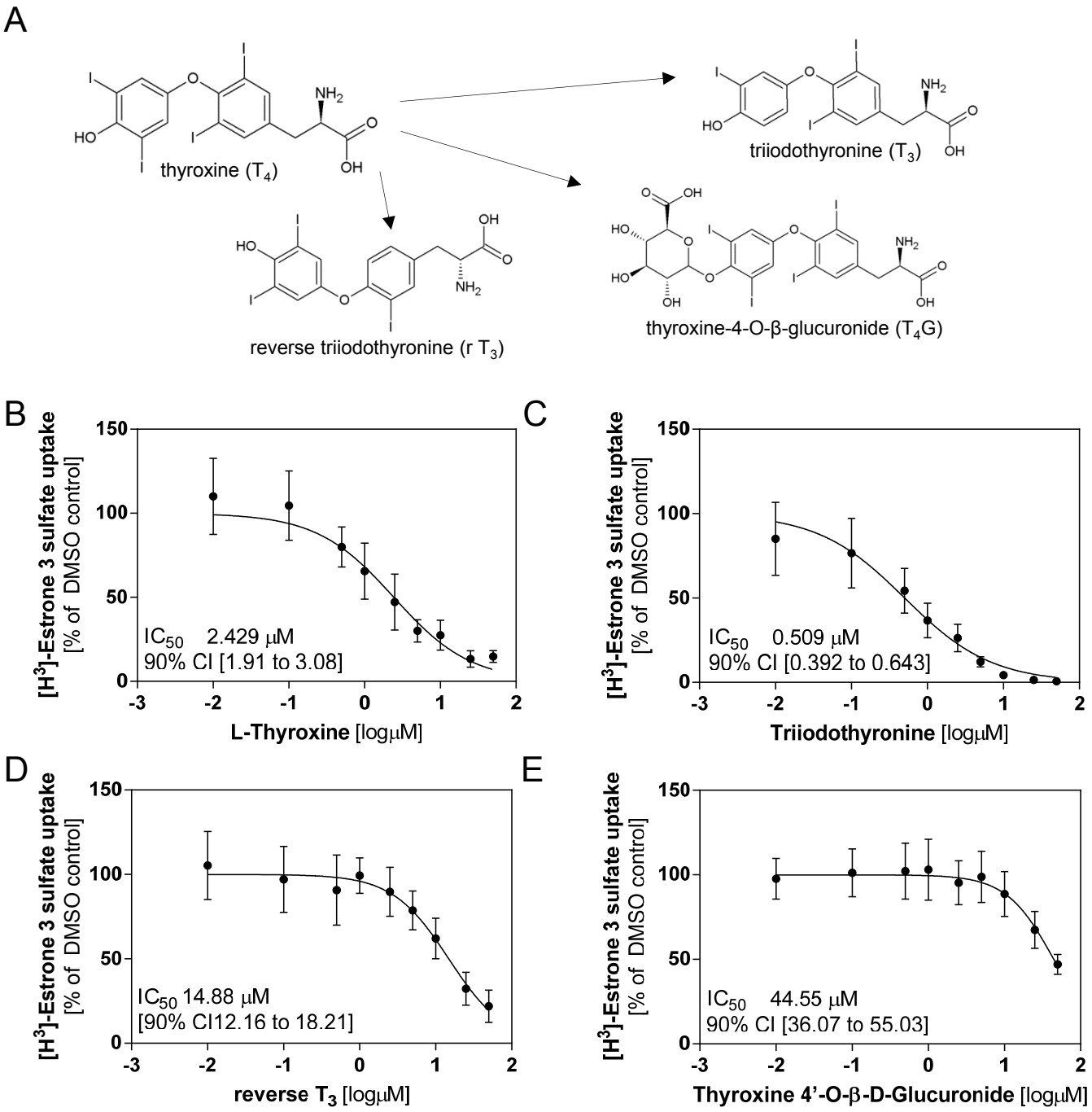

Downloaded from molpharm.aspetjournals.org at ASPET Journals on April 18, 2024

Molecular Pharmacology Fast Forward. Published on May 7, 2018 as DOI: 10.1124/mol.117.111161
This article has not been copyedited and formatted. The final version may differ from this version.

Figure 3

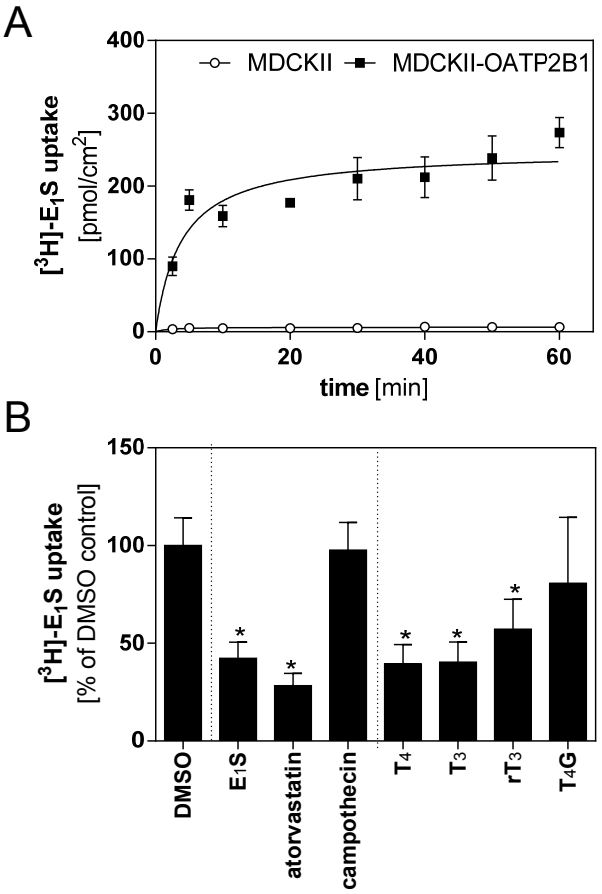

Downloaded from molpharm.aspetjournals.org at ASPET Journals on April 18, 2024

Molecular Pharmacology Fast Forward. Published on May 7, 2018 as DOI: 10.1124/mol.117.111161
This article has not been copyedited and formatted. The final version may differ from this version.

Figure 4

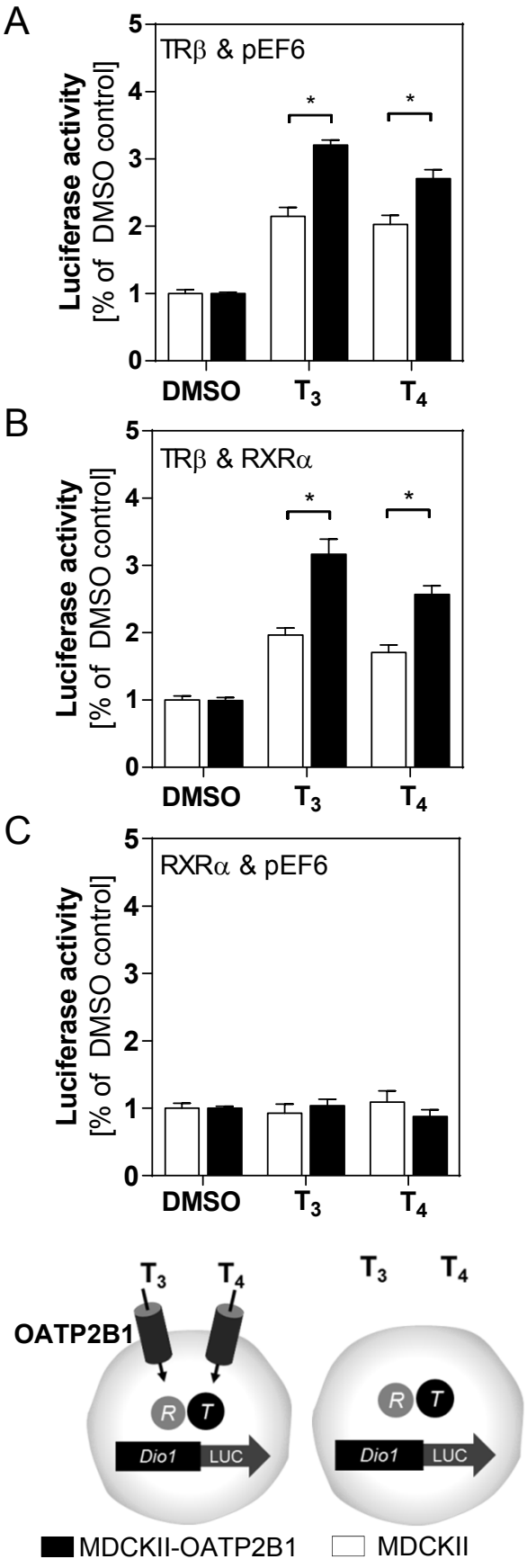

Downloaded from molpharm.aspetjournals.org at ASPET Journals on April 18, 2024

Molecular Pharmacology Fast Forward. Published on May 7, 2018 as DOI: 10.1124/mol.117.111161
This article has not been copyedited and formatted. The final version may differ from this version.

Figure 5

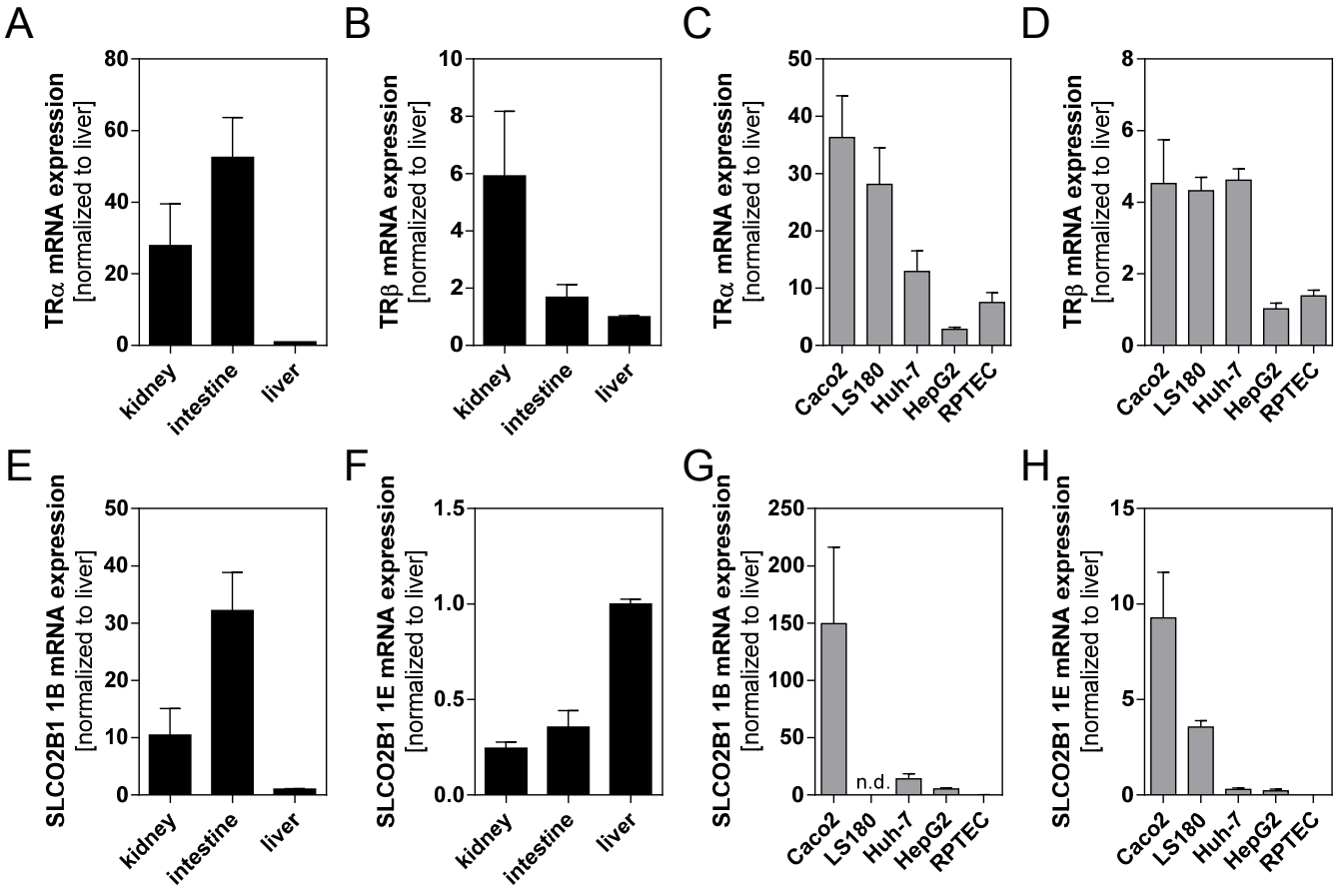

Downloaded from molpharm.aspetjournals.org at ASPET Journals on April 18, 2024

Molecular Pharmacology Fast Forward. Published on May 7, 2018 as DOI: 10.1124/mol.117.111161
This article has not been copyedited and formatted. The final version may differ from this version.

Figure 6

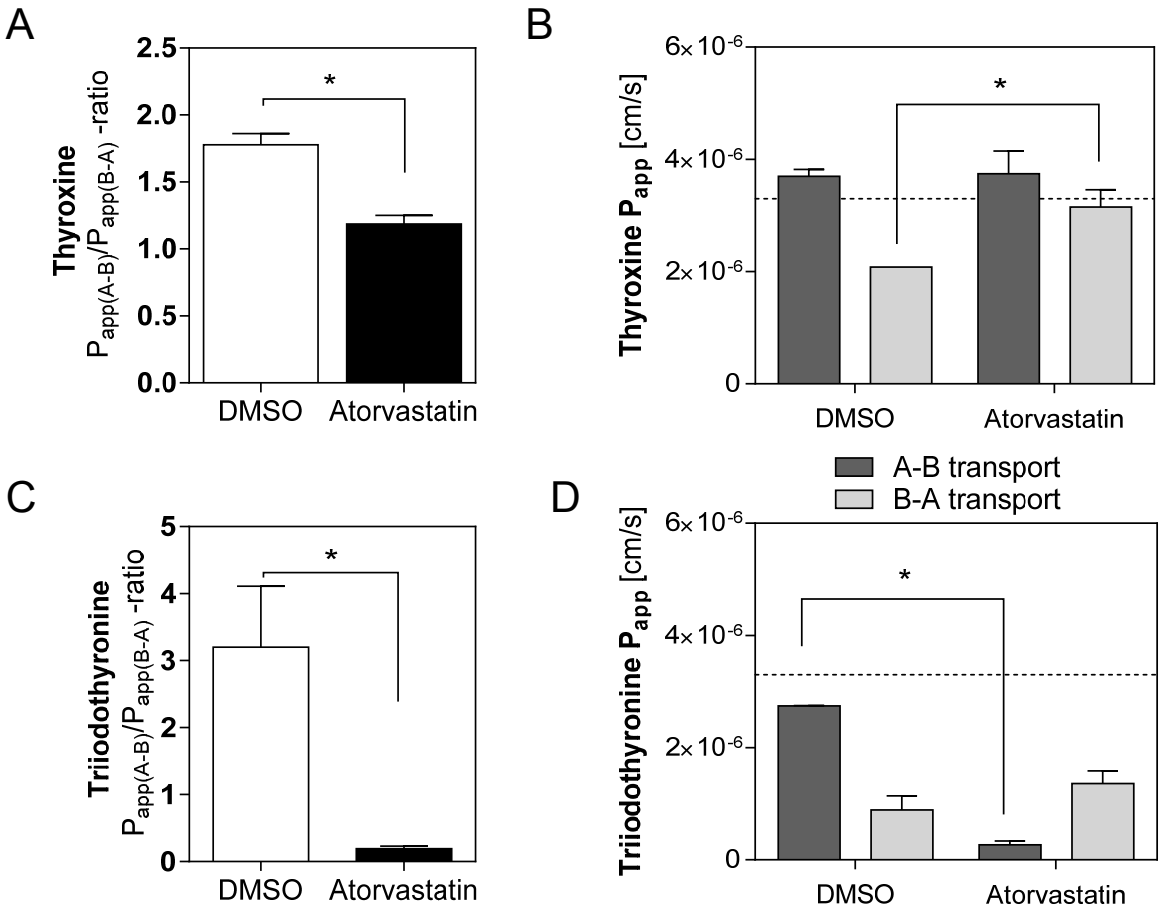

Downloaded from molpharm.aspetjournals.org at ASPET Journals on April 18, 2024

Molecular Pharmacology Fast Forward. Published on May 7, 2018 as DOI: 10.1124/mol.117.111161
This article has not been copyedited and formatted. The final version may differ from this version.

Figure 7

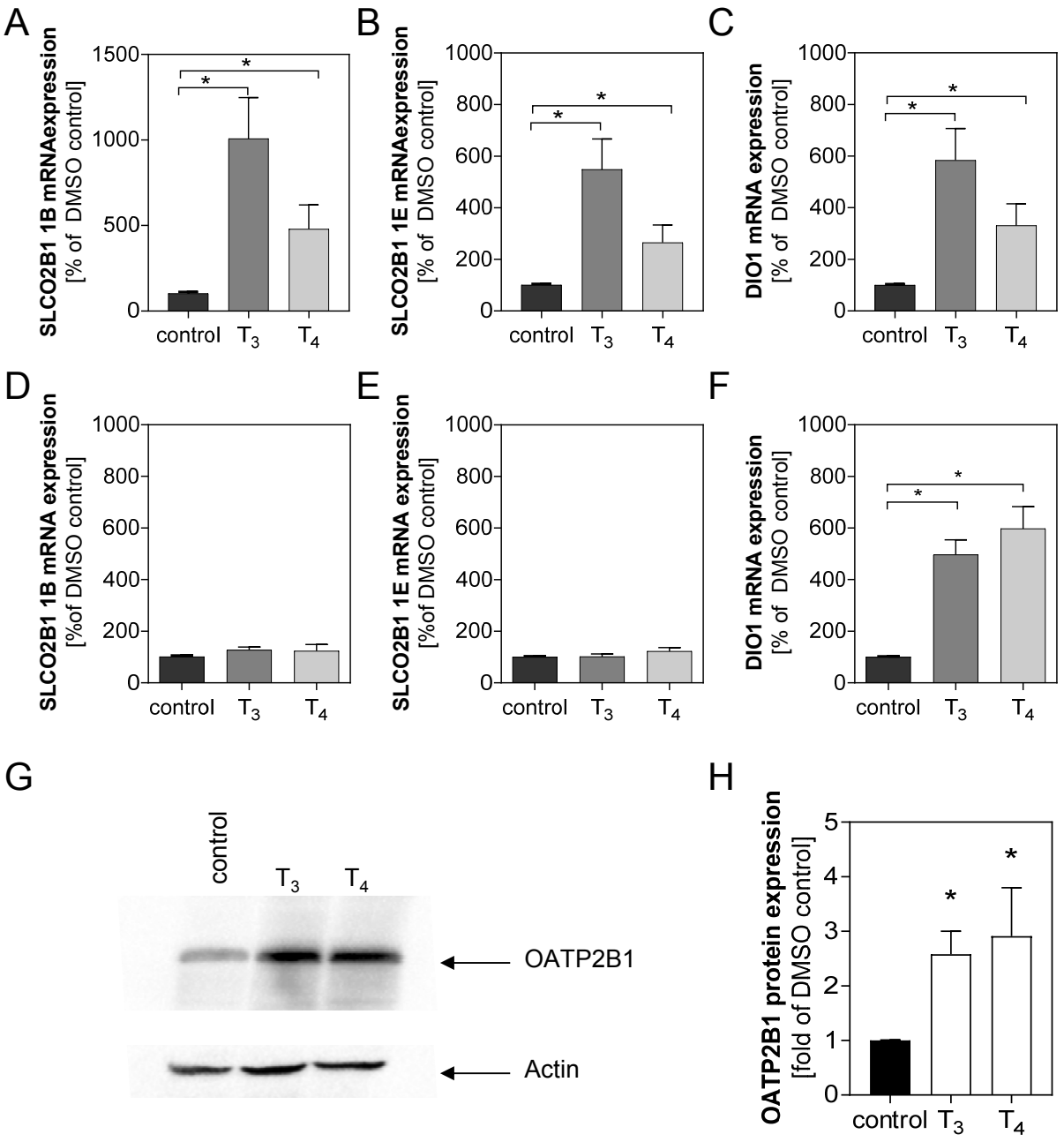

Downloaded from molpharm.aspetjournals.org at ASPET Journals on April 18, 2024

Molecular Pharmacology Fast Forward. Published on May 7, 2018 as DOI: 10.1124/mol.117.111161
This article has not been copyedited and formatted. The final version may differ from this version.

Figure 8

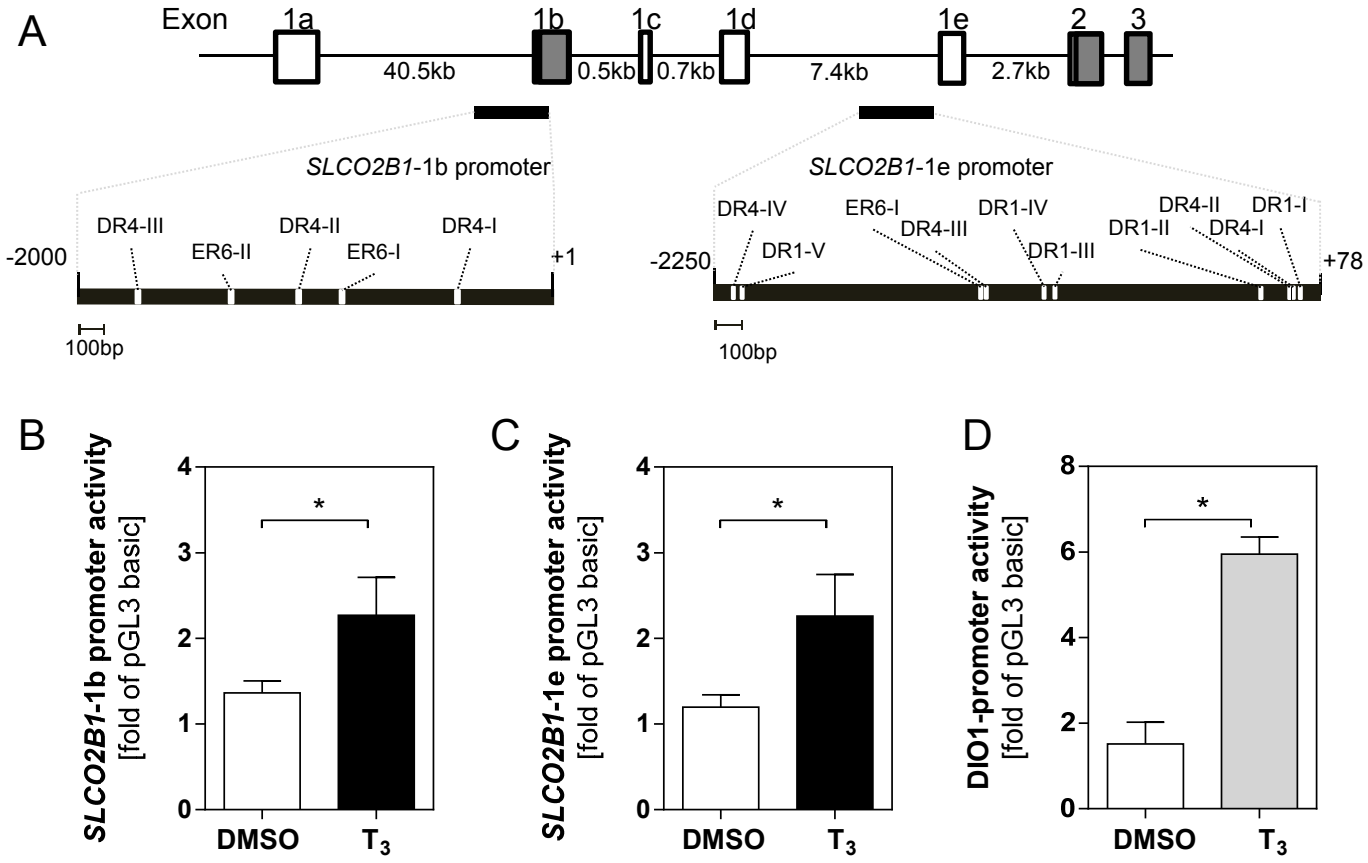

Downloaded from molpharm.aspetjournals.org at ASPET Journals on April 18, 2024